Nature Communications

https://doi.org/10.1038/s41467-026-70629-3

Article in Press

# A conserved, immune-regulated peritrophin promotes *Vibrio cholerae* colonization of the arthropod intestine

Received: 27 June 2025

Accepted: 24 February 2026

Cite this article as: Barraza, D., Paulo, T.F., Findley, L. *et al.* A conserved, immune-regulated peritrophin promotes *Vibrio cholerae* colonization of the arthropod intestine. *Nat Commun* (2026). https://doi.org/10.1038/s41467-026-70629-3

Daniela Barraza, Tânia F. Paulo, Lauren Findley, Saiyu Hang & Paula I. Watnick

# A conserved, immune-regulated peritrophin promotes *Vibrio cholerae* colonization of the arthropod intestine

Daniela Barraza[1,2¥], Tânia F. Paulo[1,3¥], Lauren Findley[1], Saiyu Hang[1,3†], and Paula I. Watnick[1,3*]

[¥] These authors contributed equally.

[1]Division of Infectious Diseases
Boston Children's Hospital
Boston, MA, USA

[2]Biological and Biomedical Sciences Program
Harvard Medical School
Boston, MA, USA

[3]Department of Pediatrics
Harvard Medical School
Boston, MA, USA

[†]Current Address:
Genentech, Inc
South San Francisco, CA, USA

*Corresponding Author:
Paula I. Watnick
Email: paula.watnick@childrens.harvard.edu

**Abstract**

*Vibrio cholerae* is a human diarrheal pathogen and an estuarine organism that associates with both terrestrial and aquatic arthropods. Using the model terrestrial arthropod *Drosophila melanogaster*, we previously showed that *V. cholerae* adheres to the arthropod intestine and activates the enteroendocrine cell innate immune response to augment expression of the enteroendocrine peptide tachykinin (Tk). Here we show that enteroendocrine innate immune signaling and Tk promote *V. cholerae* colonization of the arthropod intestine. To investigate this, we measure the impact of $Tk^{RNAi}$ on intestinal gene expression. In addition to decreasing expression of antimicrobial peptides and lipases, $Tk^{RNAi}$ reduced the expression of chitinases and chitin-binding proteins including the small, secreted chitin-binding protein Peritrophin-15a (Peri-15a). Peri-15a interacts with chitin fibrils in the peritrophic matrix, a protective coating that overlies the arthropod intestinal epithelium. We uncover that Peri-15a is essential for robust *V. cholerae* colonization of the gut. Homologs of Peri-15a are widespread in both terrestrial and aquatic organisms including marine non-biting midges, marine copepods, rotifers, and cyanobacteria. We propose that *V. cholerae* activation of the enteroendocrine cell innate immune response and Peri-15a expression represents a strategy to maximize colonization of the arthropod host intestine.

## Introduction

*Vibrio cholerae* is best known as a human pathogen that causes the diarrheal disease cholera due to expression of the principal virulence factors, the toxin co-regulated pilus and cholera toxin (1). However, both toxigenic and non-toxigenic strains of *V. cholerae* are found in estuarine aquatic environments (2-5). In these environments, *V. cholerae* is found in association with large and small marine arthropods including midges, rotifers, copepods, and cladocerans (4-7). The exoskeletons of these organisms are rich in chitin, and it has been suggested that the ability of *V. cholerae* to attach to, degrade, and grow on chitin contributes to this environmental association (8-12). Chitin also activates natural competence in *V. cholerae*, thus promoting horizontal transfer of genetic material, which is likely important to environmental adaptation and survival (13, 14).

*Drosophila melanogaster*, the common fruit fly and model arthropod, has revealed novel aspects of the interaction of *V. cholerae* with both the arthropod and mammalian intestinal epithelia (15-23). The *Drosophila* intestine consists of a foregut, midgut, hindgut and rectum (Fig 1A). The midgut is the principal site of digestion and absorption of nutrients, much like the mammalian small intestine. The midgut epithelium is separated from the intestinal contents by a porous peritrophic matrix (PM) (24). The PM consists of a lumen-exposed, web-like structure comprised of chitin and chitin-binding proteins, some of which are termed peritrophins, and an inner layer of mucins that are anchored to the chitin (25). The midgut is divided into the cardia and anterior midgut (AMG), where most of the microbiota reside, the acidic middle midgut, and the posterior midgut (PMG), which is relatively microbe-free (26). Because microbes entering the midgut first encounter the AMG, the innate immune response in this region is critical for intestinal defense. Cell types in the midgut include enterocytes with interspersed intestinal stem cells and

enteroendocrine cells. Enterocytes absorb nutrients from the diet, stem cells replenish the intestinal epithelium as needed, and enteroendocrine cells release packets of small regulatory peptides known as enteroendocrine peptides in response to luminal and systemic host signals. Enteroendocrine cells in the AMG are specialized for responding to microbial metabolites such which may signal the presence of viable microbes in the gut (27-29).

Each cell type in the intestinal epithelium encodes components of the innate immune immunodeficiency (IMD) pathway (Fig 1B) (30). The IMD pathway responds to microbial signals such as peptidoglycan, by phosphorylating and cleaving the transcription factor Relish (Rel). The N-terminus of Rel then translocates to the nucleus where it activates transcription of antimicrobial peptides (AMPs) such as Diptericin A (DptA), Attacin A (AttA), and Cecropin A1 (CecA1) (31). Enteroendocrine cells of the AMG that express the enteroendocrine peptide Tachykinin (Tk) also activate IMD signaling in response to small molecules such as acetate and tryptophan (19, 28, 29). In these cells, IMD signaling activates transcription of *Tk*, which promotes intestinal lipid utilization in addition to AMP expression (29, 32). In the absence of an invasive intestinal infection, the response of the intestine to microbes is principally under the control of enteroendocrine cells and Tk (27).

*Drosophila* ingestion of *V. cholerae* results in the formation of a biofilm in the PMG without further invasion and activates IMD signaling in enteroendocrine cells leading to an increase in intestinal Tk and AMP expression (17, 19, 28). Here we report that, despite the susceptibility of *V. cholerae* to AMPs, innate immune signaling and Tk expression in enteroendocrine cells increases *V. cholerae* colonization of the arthropod intestine. To understand how Tk regulates *V. cholerae* colonization, we compared gene expression in

the intestines of control and *Tk* knockdown flies using RNA-seq analysis. In addition to the known impacts on genes encoding AMPs and lipid catabolism enzymes, we found that Tk activates transcription of genes encoding chitin modification and chitin-binding proteins. We demonstrate that expression of a small, abundant chitin-binding protein, Peritrophin-15a (Peri-15a), which consists of a secretion peptide and one type 2 chitin-binding domain, is induced by *V. cholerae* infection and increases *V. cholerae* adhesion to the arthropod intestine.Underscoring the environmental relevance of our findings, the literature suggests that association of *Vibrio* species with zooplankton activates both the innate immune response and transcription of chitin-binding proteins (33). Furthermore, AlphaFold predictions show that close structural homologs of Peri-15a are present in many organisms that associate with *V. cholerae* in the environment including copepods, rotifers, cyanobacteria, non-biting midges, and house flies (34). Based on these findings, we propose that *V. cholerae* activation of the host enteroendocrine innate immune response may augment colonization of the intestinal surface of environmental arthropod hosts.

## Results

**The enteroendocrine innate immune response enhances *V. cholerae* colonization of the arthropod intestine.** We previously showed that *V. cholerae* infection activates intestinal IMD signaling in enteroendocrine cells leading to increased AMP transcription in the arthropod intestine (19, 29). We hypothesized that this response to *V. cholerae* infection would limit intestinal colonization. To test this, we used a Gal4/UAS binary system to generate flies carrying the yeast transcriptional activator Gal4 fused to a sequence that drives gene expression to Tk-expressing enteroendocrine cells (Tk>) and RNAi's targeting various genes fused to the upstream activating sequence to which Gal4 binds (Gene$^{RNAi}$) (35). As a control for background, we used Tk> flies crossed to the parental stock into which the RNAi constructs were inserted (36). We first fed *V. cholerae* to Tk> and Tk>*Rel*$^{RNAi}$ flies for 48 hours and then washed out non-adherent bacteria by transferring the flies to phosphate-buffered saline (PBS) for 24 hours. Unexpectedly, *Rel*$^{RNAi}$ in Tk-expressing cells decreased *V. cholerae* colonization, suggesting that IMD signaling in Tk-expressing enteroendocrine cells promotes intestinal colonization (Fig 1C). IMD signaling in enteroendocrine cells is essential for Tk expression in the AMG (29). To test the role of Tk in this process, we measured *V. cholerae* colonization in Tk>*Tk*$^{RNAi}$ flies and again observed a decrease in colonization (Fig 1D). Tk communicates with enterocytes via the TkR99D receptor (28, 32). To test whether colonization was brought about by an enterocyte-specific product, we used the enterocyte driver Myo31DF-Gal4 (NP1>) and TkR99D-specific RNAi to knock down TkR99D in enterocytes and compared colonization of NP1> and NP1>*TkR99D*$^{RNAi}$ flies. *TkR99D*$^{RNAi}$ in enterocytes increased *V. cholerae* colonization, as did *Rel*$^{RNAi}$ (Figs. 1E and F). Since enterocytes are an important source of AMPs, we reasoned that decreased IMD signaling in these

cells and, therefore, AMP production might explain the observed increase in *V. cholerae* colonization of NP1>*TkR99D*$^{RNAi}$ and NP1>*Rel*$^{RNAi}$ flies. We compared *V. cholerae* colonization of flies with 10 AMPs deleted (ΔAMP10, Def$^{SK3}$, AttC$^{Mi}$, DroAttAB$^{SK2}$, Mtk$^{R1}$, DptAB$^{SK1}$; Drs$^{R1}$, AttD$^{SK1}$) with the parental control (Fig 1G) (37). As predicted, the ΔAMP10 flies displayed increased colonization. We conclude that AMPs diminish *V. cholerae* intestinal colonization, that a Tk-regulated product of enteroendocrine cells promotes *V. cholerae* intestinal colonization, and that *V. cholerae* intestinal colonization of the arthropod intestine is a composite of these two opposing processes.

**The PM protein Peritrophin-15a is activated by Tk and the enteroendocrine innate immune response.** To identify host colonization factors regulated by Tk, we performed RNA-seq on the intestines of Tk>*Tk*$^{RNAi}$ and Tk> driver-only flies (Fig 2A and Supplementary Data 1). Using a padj ≤0.05 and 2-fold change as thresholds, we identified 136 differentially regulated genes of which transcription of 69 were increased and transcription of 67 were decreased. Tk is known to regulate both innate immune signaling and lipid catabolism (29, 32). RNA-seq analysis showed 20 differentially regulated genes involved in innate immunity (dark green circles, Fig 2A and Supplementary Data 1) and 9 involved in lipid catabolism (brown circles, Fig 2A and Supplementary Data 1) (38). To independently confirm a subset of these, we measured transcription of the genes encoding the AMP Defensin (Def) and the lipases CG17192 and Lipase 3 (Lip3) by qRT-PCR, which corroborated the RNA-seq results (Fig 2B). Opposite regulation of the two lipase genes *CG17192* and *Lip3* was unexpected, so we compared lipid accumulation in the intestines of Tk> and Tk>*Tk*$^{RNAi}$ flies. As previously reported, lipid accumulation was observed in the intestines of Tk>*Tk*$^{RNAi}$ flies (Figs. 2C and D) (32). Importantly, this was only observed in the AMG but not in the PMG. Since

Tk is present in both the AMG and PMG, we conclude that control of lipid accumulation is specific to the AMG Tk (29, 32).

In addition to genes encoding metabolic, regulatory, and unknown functions, we noted four genes (*CG10725*, *Peritrophin-15a*, *Peritrophin-15b*, and *Idgf3*) annotated as encoding chitin-binding proteins, three of which were significantly activated by Tk and one of which was repressed (Supplementary Data 1). Chitin-binding proteins are structural components of the PM, the protective layer of the intestine closest to the lumen where *V. cholerae* is located during infection (39). Previous publications suggested that disruption of the PM increased the susceptibility of *Drosophila* to intestinal bacteria and yet we observed a decreased burden of *V. cholerae* with $Tk^{RNAi}$ (40). Nevertheless, we hypothesized, that a chitin-binding protein might enhance pathogen colonization if it promoted adhesion to the PM surface. A previous study in the tsetse fly showed that the peritrophins Pro 1 and 2, which are homologs of the *Drosophila* Peritrophins-15a and b (Peri-15a and b), have little impact on the structure of the PM and do not affect colonization of the intestine by the Gram-negative rods *Enterobacter* and *Serratia* (41). Because the transcript abundance of *Peri-15a* and *Peri-15b* was significantly decreased in the Tk>$Tk^{RNAi}$ RNA-seq analysis as compared with the Tk> control, we reasoned they might be the Tk-regulated *V. cholerae* adhesion factor we sought. Peri-15a and 15b are homologous proteins consisting of 92 aa and 93 aa, respectively. They are encoded in neighboring regions of the second chromosome and, therefore, may be the product of a gene duplication. An alignment using Clustal Omega showed that they are 45% identical and 58% similar (Fig 3A) (42). AlphaFold predicts very similar structures for the two proteins, which consist of an N-terminal signal peptide and one type 2 chitin binding domain (Fig 3B) (34, 43). The *Peri-15a* transcript is most highly expressed in

enteroendocrine cells of the AMG, and is approximately 40X and 750X more highly expressed, respectively, than *Peri-15b* and *Peritrophin A*, the other two named peritrophins in the *Drosophila* genome (Fig 3C) (30). Therefore, we focused our studies on Peri-15a. We first confirmed our RNA-seq results with an independent qRT-PCR experiment comparing *Peri-15a* transcription in the intestines of Tk>*Tk*$^{RNAi}$ flies and Tk> flies. As expected, knockdown of *Tk* resulted in decreased transcript abundance of *Peri-15a* (Fig 3D). Tk>*Rel*$^{RNAi}$ also decreased *Peri-15a* transcript abundance, demonstrating that *Peri-15a* transcription is activated by IMD signaling (Fig 3E).

**Peri-15a expression is increased by *V. cholerae* infection and promotes colonization.** We next measured transcription of *Tk* and *Peri-15a* in the setting of *V. cholerae* infection. This significantly increased transcription of both *Tk* and *Peri-15a* (Fig 4A). We then assessed the impact of Peri-15a on *V. cholerae* colonization. Considering that other enteroendocrine cells might produce Peri-15a in addition to Tk-expressing ones, we knocked down *Peri-15a* transcription using the pan-enteroendocrine cell driver prospero (pros>) and *Peri-15a*$^{RNAi}$. *Peri-15a*$^{RNAi}$ reduced *V. cholerae* colonization of the *Drosophila* intestine by approximately 100-fold (Fig 4C) and decreased intestinal *Peri-15a* transcription 2-fold but did not alter transcription of *Tk* or the gene encoding the AMP *Def* (Fig 4D). To further rule out an effect of Peri-15a on Tk expression, we performed Tk and lipid staining on the intestines of pros> and pros>*Peri-15a*$^{RNAi}$ flies. pros>*Peri-15a*$^{RNAi}$ had no impact on intestinal lipid accumulation (Fig 4E and F and Fig S1). A minimal decrease in numbers of Tk+ cells was observed in the AMG only. This suggests Tk is upstream of Peri-15a and that decreased colonization of the pros>*Peri-15a*$^{RNAi}$ intestine is not the result of increased AMP transcription.

**Dietary ecdysone increases *V. cholerae* colonization of the arthropod gut**. We previously showed that the fly steroid hormone 20-hydroxyecdysone (20E) activates the intestinal innate immune response and Tk expression (28). We hypothesized that intestinal *Peri-15a* expression would, therefore, be activated by dietary supplementation with 20E. To test this, we compared *Tk* and *Peri-15a* transcription in the intestines of flies fed LB alone or supplemented with 20E. As shown in Figure 5A, administration of 20E to *Drosophila* increased expression of *Tk* and *Peri-15a*. Furthermore, 20E administration increased intestinal colonization by *V. cholerae* (Fig 5B). To demonstrate that this increase in colonization was correlated with Peri-15a expression, we assessed the impact of 20E on *V. cholerae* colonization in pros> and pros>*Peri-15a*$^{RNAi}$ flies. Supplementation with 20E increased colonization of pros> flies but did not significantly increase *V. cholerae* colonization in pros>*Peri-15a* flies (Fig 5C). This demonstrates that the increased colonization observed with 20E supplementation is dependent on Peri-15a and further supports our contention that Peri-15a directly promotes host colonization.

**Decreasing the porosity of the PM chitin layer does not increase *V. cholerae* colonization**. Peri-15a has a single chitin-binding domain and is, therefore, hypothesized to be a capping protein that limits the length of chitin strands in the PM (44). We reasoned that *Peri-15a*$^{RNAi}$ might alter the porosity of the PM. To independently test the impact of increasing the porosity of the PM surface on *V. cholerae* colonization, we examined intestinal chitinases. In the cotton bollworm, silencing of the *Cht4* homolog results in a less porous PM with a higher chitin content (45). *Cht4* and *Cht9*, which are the most highly expressed chitinases in the midgut, are principally expressed in enteroblasts and enterocytes of the *Drosophila* midgut (46) (Fig 6A). To determine how they impact *V. cholerae* colonization, we compared *V. cholerae* colonization of NP1>*Cht4*$^{RNAi}$ and

NP1>*Cht9*$^{RNAi}$ flies with NP1> flies. *Cht9*$^{RNAi}$ had no effect on *V. cholerae* colonization, while *Cht4*$^{RNAi}$ unexpectedly decreased colonization (Fig 6B). It was surprising that decreased PM porosity and increased chitin content would inhibit *V. cholerae* colonization directly, since chitin has been shown to promote *V. cholerae* surface adhesion (12, 47, 48). Studies on Tsetse flies have suggested that decreased PM porosity diminishes access of microbial products to the intestinal epithelium and, thus, reduces IMD signaling (41). Based on this precedent, we hypothesized that decreased PM porosity in NP1>*Cht4*$^{RNAi}$ flies might decrease IMD signaling and, consequently, *Tk* and *Peri-15A* expression. To test this, we quantified transcription of *Cht4*, *Tk*, *Def*, and *Peri-15a* in the intestines of NP1>*Cht4*$^{RNAi}$ and NP1> flies (Fig 6C) and found that all four transcripts were decreased by *Cht4*$^{RNAi}$. These findings are consistent with a model in which *Cht4*$^{RNAi}$ reduces access of microbial products to the intestinal epithelium leading to decreased IMD signaling and *Peri-15a* transcription and does not support a model in which continuity of the PM promotes *V. cholerae* colonization.

**Peri-15a is not essential to maintain PM integrity.** We questioned whether *Peri-15a*$^{RNAi}$ might alter the permeability of the PM. Penetration of ingested FITC-labelled dextran into intestinal cells has previously been used to demonstrate the essential role of the chitin-binding protein Crystallin (Crys) in PM integrity (40). We, therefore, used 40kDa and 500kDa FITC-labelled dextran to assess the permeability of the PMs of pros> and pros>*Peri-15a*$^{RNAi}$ flies, including the *Crys*$^{MB08319}$ mutant as a positive control, and NP1>*Cht4*$^{RNAi}$ flies as a negative control (Fig 7). As proof of principle, no leakage of either the 40 kDa- and 500 kDa FITC-labelled dextran was observable for NP1> and NP1>*Cht4*$^{RNAi}$ flies, while clear leakage of both the 40 kDa- and 500 kDa FITC-labelled dextran was observed with the *Crys*$^{MB08319}$ mutant. As compared with the positive control,

there was no leakage in either pros> or pros>*Peri-15a*$^{RNAi}$ fly intestines with either the 40 kDa- and 500 kDa FITC-labelled dextran. We conclude that, unlike Crys, Peri-15a is not essential for the integrity of the PM.

Interestingly, we noted a difference in the distribution of the 40 kDa FITC-labelled dextran in the PMG of several of the pros>*Peri-15a*$^{RNAi}$ intestines consistent with a filling defect (Fig 7 and S2). This difference was less apparent with the 500 kDa FITC-labelled dextran. We hypothesize that Peri-15a may increase the rigidity or decrease the elasticity of the PM. However, we cannot rule out a differential response to the fixation step in our sample preparation.

**The global chitin-responsive transcription factor ChiS is active in the arthropod intestine and reduces *V. cholerae* colonization**. *V. cholerae* can use chitin as a sole carbon and nitrogen source because its genome encodes multiple chitinases as well as transporters and enzymes that enable catabolism of chitin degradation products (12, 49-51). The latter *V. cholerae* chitin catabolic cascade is under the control of the non-canonical transcription factor ChiS (12, 50, 52). We previously showed that *V. cholerae* is able to digest the *Drosophila* PM, suggesting that ChiS is active in the *Drosophila* intestine (53). To demonstrate this, we measured expression of *chiA1* and *chiA2*, two chitinase-encoding genes in the ChiS regulon, in the intestines of flies infected either with WT *V. cholerae* or a Δ*chiS* mutant. As shown in Fig 8A, deletion of *chiS* reduced expression of both genes, suggesting that ChiS is active in the arthropod intestine.

Chitin and, therefore, ChiS is thought to be critical for growth of *V. cholerae* in the presence of arthropods (5, 9, 49, 54). Our results show that the host chitin-binding protein Peri-15a promotes *V. cholerae* colonization of the arthropod gut. We, therefore,

questioned how *V. cholerae* degradation of chitin in the arthropod gut might modulate colonization and assessed colonization by WT *V. cholerae* and a *V. cholerae* Δ*chiS* mutant. Mutation of chiS had a small but reproducible positive effect on colonization in a control fly (Fig 8B). This suggests that metabolism of chitin is not essential for *V. cholerae* colonization of the arthropod intestine. We reasoned, instead, that chitin degradation might damage the PM leading to increased IMD signaling and AMP expression. To test this directly, we compared colonization by WT *V. cholerae* and a Δ*chiS* mutant in the ΔAMP fly. The increased colonization of the Δ*chiS* mutant was preserved in the ΔAMP fly background, suggesting that this difference does not rely on a difference in AMP expression. We then questioned whether improved colonization by the Δ*chiS* mutant was dependent on Tk and Peri-15a. As shown in Figs 7C and D, in Tk>*Tk*$^{RNAi}$ and pros>*Peri-15a*$^{RNAi}$ flies, the Δ*chiS* mutant no longer had a colonization advantage over WT *V. cholerae*. One possibility is that *V. cholerae* chitin catabolism removes Peri-15a from the PM via degradation of chitin attachment sites, thus decreasing colonization of the arthropod intestine.

**Peri-15a is broadly conserved in insects and marine zooplankton.** *V. cholerae* has been associated with zooplankton in aquatic environments, and there is evidence that *V. cholerae* colonizes these organisms using specific adhesins (5, 55-60). Furthermore, transcription of copepod genes encoding innate immune effectors and chitin binding proteins, including a homolog of Peri-15a, are increased in response to *Vibrio* colonization (33). To understand the relevance of our findings to the natural environment of *V. cholerae*, we searched for structural homologs of Peri-15a in the AlphaFold protein structure database. Highly similar Peri-15a homologs were present in diverse insects including mosquitos, beetles, butterflies, and sand flies (Fig 8).

Structural homologs of Peri-15a were also identified in the genomes of marine non-biting midges, rotifers, marine copepods, and fungi, all of which are found in the marine aquatic environments inhabited by *V. cholerae*. Taken together, these results suggest that Peri-15a homologs are present in natural environmental hosts of *V. cholerae* and that intestinal colonization with *V. cholerae* increases expression of these proteins.

## Discussion

Arthropods figure prominently in the environmental life cycle of *V. cholerae*. Here we show that a small, widely conserved arthropod protein consisting of a secretion peptide and a single type 2 chitin binding domain promotes *V. cholerae* colonization of the arthropod intestine. This protein, termed Peri-15a in the model arthropod *Drosophila melanogaster*, is regulated by the enteroendocrine peptide Tk, expressed almost exclusively in enteroendocrine cells of the adult midgut, and secreted and incorporated into the PM. Homologs of Peri-15a are widely distributed in terrestrial arthropods and zooplankton that have been associated with *V. cholerae*. While the goal of increasing Peri-15a expression may be to protect the PM from microbial degradation, we propose that *V. cholerae* has co-opted Peri-15a as an intestinal colonization factor of environmental arthropod hosts.

Environmental studies suggest that the presence of *V. cholerae* in the water column is correlated with zooplankton such as cladocerans, copepods, and rotifers (5, 61, 62). Attachment to the exoskeletons of zooplankton has also been observed in the laboratory (10, 56, 59). Arthropods, which include cladocerans and copepods, have been found to dominate the zooplankton population in diverse environments (63-67). In the laboratory, some have observed that *V. cholerae* attaches much more abundantly to dead zooplankton or their molts as compared with live ones (57, 60). This is not surprising as the arthropod exoskeleton is designed to be an impermeable, microbe-resistant barrier (68). The outermost layer is comprised of hydrophobic lipoproteins, while inner layers consist of complex bundles of protein-chitin fibers. Thus, shed exoskeletons provide more ready access to chitin. In contrast, the intestine of arthropods provides a more protected environment for microbes such as *V. cholerae*, which have been found in the

intestines of zooplankton (22, 69). While the exoskeleton is impermeable, the PM of the midgut, with its thin and readily accessible chitin fibers, is designed for permeability as it must allow transit of nutrients and small molecules (70). Here we provide evidence for a specific interaction between *V. cholerae* and a protein incorporated into the arthropod PM.

PM porosity has been shown to modulate the burden of intestinal bacteria in other insects. PM porosity is critical because it must balance permeability to nutrients, which is essential, with permeability to microbe or microbe metabolism-associated molecular products, which may lead to chronic immune stimulation and intestinal damage. Consistent with this model, *Cht4* knockdown in the insect *Helicoverpa armigera* decreased PM porosity and body weight (45). Furthermore, in the tsetse fly, investigators found that chitin synthase knockdown activated the intestinal innate immune response, presumably by increasing PM permeability. This reduced the intestinal burden of orally administered Gram-negative pathogens such as *Serratia marcescens* and *Enterobacter* sp (41). Large PM proteins have multiple chitin binding domains that are thought to crosslink single chitin fibers to each other to form fibrils that provide structural rigidity to the matrix (25). In contrast, Peri-15a consists of only one chitin binding domain. Biochemical studies have shown that Peri-15a binds chitin directly at very low stoichiometry *in vitro* and is tightly associated with the PM (44). Therefore, rather than crosslinking chitin fibers, it has been suggested that Peri-15a is a capping protein that protects single chitin strands from exochitinases. Homologs of Peri-15a and b, known as Proventriculin 1 and 2, have been identified and studied in the PM of the tsetse fly (71). Consistent with the model of Peri-15a as a capping protein, these studies and ours found that knockdown of these proteins left the permeability of the PM largely intact (41).

Therefore, it is unlikely that Peri-15a promotes *V. cholerae* colonization through a major change in PM permeability.

Here, we report that knockdown of *Cht4*, which is predicted to reduce matrix porosity, decreased the intestinal innate immune response, expression of *Peri-15a*, and intestinal colonization by *V. cholerae*. In contrast to *Drosophila* chitinase *Cht4*, deletion of *V. cholerae chiS*, the master regulator of *Vibrio* chitin catabolism, increased colonization of the arthropod intestine (12, 52, 72). ChiS activates transcription of genes encoding at least four of the five proven *Vibrio* endochitinases: chiA1 (VC1952), ChiA2 (VCA0027), VC0769, and VCA0700 (11, 12), and we have previously presented evidence that *V. cholerae* thins the chitinous layer of the *Drosophila* PM, suggesting that these chitinases are active in the *Drosophila* intestine (53). Knockdown of arthropod chitinases decreases the porosity of the PM and expression of *Peri-15a*. In contrast, *V. cholerae* chitinases act on naturally formed PMs to digest them, possibly depleting Peri-15A at the same time. It has previously been proposed that *V. cholerae* attaches to and degrades environmental chitin to release nutrients required for its growth (9). Our results suggest that degradation of chitin by *V. cholerae* promotes detachment from the chitin-rich PM and may actually represent a means of dispersal into the environment. Taken together, these findings support a model in which Peri-15a does not enhance *V. cholerae* intestinal colonization by altering PM porosity. Rather, we propose that Peri-15a either binds a *V. cholerae* adhesin directly or reveals a binding site in the PM for such an adhesin.

GbpA (VCA0811) and FrhA (VC1620) are two *V. cholerae* adhesins that mediate binding to abiotic surfaces, plankton and the mammalian intestinal epithelium(55, 56). GbpA is a secreted, four-domain 485aa protein whose expression is increased by chitin but which, unlike the *V. cholerae* chitinases, is not under ChiS control (12, 73). Domains

1 and 4 mediate chitin binding, domain 1 also mediates binding to mammalian mucins, and domains 2 and 3 interact with the *V. cholerae* surface, enabling GbpA to form bridges between the bacterium and other surfaces (73). While biochemical studies have shown that GbpA can function as a chitinase, there is no *in vivo* evidence for this as of yet (11, 74). FrhA is a secreted 2,251 amino acid protein first identified because it was co-regulated with the flagellar apparatus (75). It contains three large N-terminal Calx-beta $Ca^{2+}$ binding domains and 4 C-terminal cadherin-like $Ca^{2+}$ binding domains. Amino acids residues 1155-1350 were recently identified as a peptide-binding domain that is sufficient to enhance binding to abiotic surfaces, epithelial cells, the mouse intestine, and diatoms (56). Either of these or a novel protein could serve as the adhesin mediating attachment to the PM via Peri-15a.

The observation that *V. cholerae* possesses all the transporters and enzymes required to utilize chitin as a sole energy source, that the *V. cholerae* genome encodes a transcription factor dedicated to regulating its interaction with chitins, and that *V. cholerae* becomes naturally competent in the presence of chitin suggest that chitinous surfaces play an important role in the *V. cholerae* life cycle (12, 13, 50). Here we provide further evidence for a specific interaction between *V. cholerae* and the arthropod intestinal PM by identifying a protein component of this matrix that does not significantly alter its permeability but, nevertheless, enhances *V. cholerae* colonization.

**Methods:**

*Drosophila* husbandry and strains. All fly stocks used in this study were raised on standard fly food containing 16.5 g/L yeast, 9.5 g/L soy flour, 71 g/L cornmeal, 5.5 g/L agar, 5.5 g/L malt, 7.5% corn syrup, and 0.4% propionic acid in a humidified 12 hr day-

night cycle incubator at 25°C. Females flies (4-7 day old) were used in all experiments. The following fly stocks were obtained from the Bloomington *Drosophila* Stock Center (BDSC): *Tk*$^{RNAi}$ (BL2500), *Rel*$^{RNAi}$ (BL28943), *TkR99D*$^{RNAi}$ (BL27513), *Cht4*$^{RNAi}$ (BL65001), *Peritrophin-15a*$^{RNAi}$ (BL55987), and pros-Gal4/Sb (BL84276). Control lines TRiP (BL36303), $y^1w^1$ (BL1495) and *Crys*$^{MB08319}$ (BL26106) were also obtained from the BDSC. The Tk-Gal4 and NP1-Gal4 driver lines were a kind gift from the Veenstra and Perrimon laboratories (32, 76). The AMP-deficient flies and the corresponding parental strain were generously provided by the Lemaitre laboratory (37).

Bacterial strains and media. The wild-type *V. cholerae* strain and the parental background for all mutants was quorum sensing-competent *V. cholerae* 01 El Tor strain C6706 (C6706 str 2), a kind gift of the late Ronald Taylor. The Δ*chiS* mutant was constructed by double homologous recombination as previously described using the primers listed in Supplementary Data 2 (18). *V. cholerae* was cultured at 27°C in LB broth (Miller formulation, Difco) or on LB agar (Difco) supplemented with 100 μg/mL streptomycin. Where noted, 20-hydroxyecdysone was added to LB broth for *Drosophila* colonization studies (10 μM, Sigma).

*V. cholerae* mutant construction. An in-frame *V. cholerae* Δ*chiS* mutant was constructed by double homologous recombination as previously described (77). ChiS is comprised of 1177 amino acids. In this mutant, residues 172 to 1053 were deleted including all conserved domains.

*V. cholerae* colonization assays. For colonization assays, *V. cholerae* was cultured overnight in LB broth and then diluted 10-fold in fresh LB broth. 3 mL of this suspension was infused into autoclaved cellulose plugs inserted at the bottom of fly vials. 4–7-day

old flies were placed in these prepared vials for 48 hours at 25 °C and then transferred to fresh vials containing cellulose plugs infused with 3 mL sterile solution of phosphate-buffered saline for 24-hours to washout non-adherent bacteria. Individual flies treated in this manner were then homogenized in 200 µL of 1x PBS using a TissueLyser III system (Qiagen). Serial 10-fold dilutions were prepared, and 20 µl of these dilutions were plated on LB agar plates supplemented with 100 µg/mL streptomycin. The plates were incubated at 27°C for 24 hours and colony-forming units (CFU) in each dilution were enumerated. This was used to calculate *V. cholerae* CFU/fly.

*Drosophila* RNA extraction, RNA-seq, and RT-qPCR. Total RNA was isolated from 10-15 fly intestines using TRIzol reagent (Thermo Fisher Scientific 15596026) and the Direct-zol RNA Miniprep plus kit (Zymo Research R2070). Three to six biological replicates per condition/genotype were performed. For RNA sequencing analysis, the RNA was submitted to the Molecular Biology Core Facilities (MBCF) at the Dana Farber Cancer Institute (DFCI) for next-generation sequencing (NGS) library preparation, sequencing, and analysis (https://mbcf.dana-farber.org/totalrnaseq.html). Roche Kapa mRNA HyperPrep strand specific sample preparation kits were used to prepare libraries on a Beckman Coulter Biomek i7 from 200ng of purified total RNA. The resulting dsDNA libraries were quantified by Qubit fluorometer and Agilent TapeStation 4200. Uniquely dual indexed libraries were pooled in an equimolar ratio and shallowly sequenced on an Illumina MiSeq to further evaluate library quality and pool balance. The final pool was sequenced on an Illumina NovaSeq X Plus targeting 40 million 150bp read pairs per library. Sequenced reads were aligned to the UCSC hg38 reference genome assembly and gene counts were quantified using STAR (v2.7.3a) and Salmon (78, 79). Differential

gene expression testing was performed by DESeq2 (v1.22.1) (80). RNAseq analysis was performed using the VIPER snakemake pipeline (81).

For qRT-PCR, the iScript™ cDNA synthesis kit (Bio-Rad 1708891) was used to synthesize cDNA from 500ng of total RNA. The iTaq™ Universal SYBR® Green Supermix (Bio-rad 1725121) was used to perform qPCR of target gene transcripts on a QuantStudio™ Real-Time PCR system 3 (Thermo Fisher Scientific). Quantification cycle values (Cq) were obtained and used to calculate target gene transcription normalized to Actin (for *D. melanogaster* genes) or to rpoA (for *V. cholerae* genes). Primers used in this study are listed in Supplementary Data 2.

FITC-labelled dextran feeding. 40 kDa- (Sigma-Aldrich FD40) and 500 kDa- (Sigma-Aldrich FD500S) labelled dextran were resuspended in a 2.5% sucrose solution and passed over PD MiniTrap™ G-10 columns (Cytiva) prior to feeding. Adult female flies were starved for 2 hours and then placed in tubes containing a thin cellulose plug with 200 µL of the dextran suspension added. The flies were given access to this suspension for 24 hours, after which their guts were dissected and prepared as stated below.

Lipid staining and immunofluorescence of *Drosophila* intestine. Fly intestines were dissected in 1x PBS and fixed in a 4% paraformaldehyde (PFA), 0.1% PBS-Tween 20 (PBT) solution for 20 minutes. For lipid staining only, the intestines were then washed three times for 10 minutes with PBT, followed by incubation in staining solution #1 (PBT + 1:1000 DAPI (Invitrogen D1306) + 1:500 BODIPY 493/503 (Invitrogen D3922)) for 2 hours. For lipid staining and Tk-immunofluorescence experiments, intestines were washed three times for 10 minutes in PBT and then left in blocking solution (PBT + 0.1% Triton X-100 (Sigma-Aldrich 9002-93-1) + 2% BSA (Sigma-Aldrich 9048-46-8)) for 1 hour.

After this blocking step, intestines were left in Rabbit anti-Tk primary antibody solution (blocking solution + 1:500 anti-Tk) overnight at 4°C. The next day the guts were washed three times with PBT for 10 minutes, followed by incubation in staining solution #2 (blocking solution + 1:1000 DAPI (Invitrogen D1306) + 1:500 BODIPY 493/503 (Invitrogen D3922) + 1:500 Alexa 594-conjugated Goat anti-rabbit secondary antibody (Thermo Fisher Scientific A11012)) for 2 hours. After incubation in the appropriate staining solution, intestines were washed three times for 10-minutes in PBT and then mounted in Vectashield® antifade mounting medium (Vector Laboratories H-1000-10). Intestines were imaged using a Zeiss LSM 980 confocal microscope using a 40X (Fig 2) or 25X (Fig 4) oil objective. Unless otherwise noted, all steps were done at room temperature. Lipid accumulation was quantified using ImageJ (FIJI) to measure total BODIPY fluorescence. The corrected total cell fluorescence (CTCF) was calculated by dividing total BODIPY fluorescence by the total area and subtracting background fluorescence from this measurement. Tk-expressing cells were quantified manually. A minimum of six fly intestines per genotype were evaluated for quantification of Tk-expressing cells and BODIPY fluorescence.

Statistical analysis and reproducibility. All data were graphed and analyzed using Prism 10.0 software (GraphPad). Measurements shown in each graph represent the mean values of at least three biological replicates for qRT-PCR, at least six flies for colonization experiments, and at least six intestines for microscopy. The mean is shown for all experiments, and error bars represent the standard deviation. Where noted, data were log-transformed to obtain a normal distribution. Appropriate statistical tests were chosen based on numbers of conditions assessed and tests of normality and variance. The

statistical test used in each graph is specified in the figure legend. With the exception of the RNA-seq, all experiments were repeated one or more times with similar results.

**Data availability statement**. Source data are provided with this paper. The RNA-seq data generated in this study have been deposited in the NCBI repository (accession no. GSE294931). Remaining raw data generated are available at doi:10.5281/zenodo.18624207

**References**


1. A. Hsiao, J. Zhu, Pathogenicity and virulence regulation of *Vibrio cholerae* at the interface of host-gut microbiome interactions. *Virulence* **11**, 1582–1599 (2020).
2. S. I. Miyoshi *et al.*, Isolation of *Vibrio cholerae* and Vibrio vulnificus from Estuarine Waters, and Genotyping of V. vulnificus Isolates Using Loop-Mediated Isothermal Amplification. *Microorganisms* **12** (2024).
3. S. K. Banerjee, R. Rutley, J. Bussey, Diversity and Dynamics of the Canadian Coastal Vibrio Community: an Emerging Trend Detected in the Temperate Regions. *J Bacteriol* **200** (2018).
4. M. L. Lizarraga-Partida *et al.*, Association of *Vibrio cholerae* with plankton in coastal areas of Mexico. *Environ Microbiol* **11**, 201–208 (2009).
5. G. C. de Magny *et al.*, Role of Zooplankton Diversity in *Vibrio cholerae* Population Dynamics and in the Incidence of Cholera in the Bangladesh Sundarbans. *Appl Environ Microbiol* **77**, 6125–6132 (2011).
6. M. Broza, H. Gancz, Y. Kashi, The association between non-biting midges and *Vibrio cholerae*. *Environ Microbiol* **10**, 3193–3200 (2008).
7. R. Sela, B. K. Hammer, M. Halpern, Quorum-sensing signaling by chironomid egg masses' microbiota, affects haemagglutinin/protease (HAP) production by *Vibrio cholerae*. *Mol Ecol* **30**, 1736–1746 (2021).
8. A. Huq *et al.*, Ecological relationships between *Vibrio cholerae* and planktonic crustacean copepods. *Appl Environ Microbiol* **45**, 275–283 (1983).
9. C. Pruzzo, L. Vezzulli, R. R. Colwell, Global impact of *Vibrio cholerae* interactions with chitin. *Environ Microbiol* **10**, 1400–1410 (2008).

10. D. A. Chiavelli, J. W. Marsh, R. K. Taylor, The mannose-sensitive hemagglutinin of *Vibrio cholerae* promotes adherence to zooplankton. *Appl Environ Microbiol* **67**, 3220–3225. (2001).

11. C. A. Hayes, T. N. Dalia, A. B. Dalia, Systematic genetic dissection of chitin degradation and uptake in *Vibrio cholerae*. *Environ Microbiol* **19**, 4154–4163 (2017).

12. K. L. Meibom *et al.*, The *Vibrio cholerae* chitin utilization program. *Proc Natl Acad Sci U S A* **101**, 2524–2529 (2004).

13. K. L. Meibom, M. Blokesch, N. A. Dolganov, C. Y. Wu, G. K. Schoolnik, Chitin induces natural competence in *Vibrio cholerae*. *Science* **310**, 1824–1827 (2005).

14. M. Blokesch, G. K. Schoolnik, Serogroup conversion of *Vibrio cholerae* in aquatic reservoirs. *PLoS Pathog* **3**, e81 (2007).

15. L. Kamareddine *et al.*, Activation of *Vibrio cholerae* quorum sensing promotes survival of an arthropod host. *Nat Microbiol* **3**, 243–252 (2018).

16. Z. Wang, S. Hang, A. E. Purdy, P. I. Watnick, Mutations in the IMD pathway and mustard counter *Vibrio cholerae* suppression of intestinal stem cell division in Drosophila. *MBio* **4**, e00337–00313 (2013).

17. A. E. Purdy, P. I. Watnick, Spatially selective colonization of the arthropod intestine through activation of *Vibrio cholerae* biofilm formation. *Proc Natl Acad Sci U S A* **108**, 19737–19742 (2011).

18. A. S. Vanhove *et al.*, *Vibrio cholerae* ensures function of host proteins required for virulence through consumption of luminal methionine sulfoxide. *PLoS Pathog* **13**, e1006428 (2017).

19. B. E. Jugder *et al.*, *Vibrio cholerae* high cell density quorum sensing activates the host intestinal innate immune response. *Cell Rep* **40**, 111368 (2022).

20. N. S. Blow *et al.*, *Vibrio cholerae* infection of *Drosophila melanogaster* mimics the human disease cholera. *PLoS Pathog* **1**, e8 (2005).

21. D. Fast, B. Kostiuk, E. Foley, S. Pukatzki, Commensal pathogen competition impacts host viability. *Proc Natl Acad Sci U S A* **115**, 7099–7104 (2018).

22. T. Xu, A. Novotny, S. Zamora-Terol, P. A. Hamback, M. Winder, Dynamics of Gut Bacteria Across Different Zooplankton Genera in the Baltic Sea. *Microb Ecol* **87**, 48 (2024).

23. D. Fast *et al.*, *Vibrio cholerae*-Symbiont Interactions Inhibit Intestinal Repair in *Drosophila*. *Cell Rep* **30**, 1088–1100 e1085 (2020).

24. A. C. Wong, A. S. Vanhove, P. I. Watnick, The interplay between intestinal bacteria and host metabolism in health and disease: lessons from *Drosophila melanogaster*. *Dis Model Mech* **9**, 271–281 (2016).

25. S. Muthukrishnan, H. Merzendorfer, Y. Arakane, Q. Yang, Chitin Organizing and Modifying Enzymes and Proteins Involved In Remodeling of the Insect Cuticle. *Adv Exp Med Biol* **1142**, 83–114 (2019).

26. H. Li, Y. Qi, H. Jasper, Preventing Age-Related Decline of Gut Compartmentalization Limits Microbiota Dysbiosis and Extends Lifespan. *Cell Host Microbe* **19**, 240–253 (2016).

27. P. I. Watnick, B. E. Jugder, Microbial Control of Intestinal Homeostasis via Enteroendocrine Cell Innate Immune Signaling. *Trends Microbiol* **28**, 141–149 (2020).

28. B. E. Jugder, L. Kamareddine, P. I. Watnick, Microbiota-derived acetate activates intestinal innate immunity via the Tip60 histone acetyltransferase complex. *Immunity* **54**, 1683–1697 e1683 (2021).

29. L. Kamareddine, W. P. Robins, C. D. Berkey, J. J. Mekalanos, P. I. Watnick, The *Drosophila* Immune Deficiency Pathway Modulates Enteroendocrine Function and Host Metabolism. *Cell Metab* **28**, 449–462 e445 (2018).

30. D. Dutta *et al.*, Regional Cell-Specific Transcriptome Mapping Reveals Regulatory Complexity in the Adult *Drosophila* Midgut. *Cell Rep* **12**, 346–358 (2015).

31. A. Kleino, N. Silverman, The *Drosophila* IMD pathway in the activation of the humoral immune response. *Dev Comp Immunol* **42**, 25–35 (2014).

32. W. Song, J. A. Veenstra, N. Perrimon, Control of lipid metabolism by tachykinin in *Drosophila*. *Cell Rep* **9**, 40–47 (2014).

33. A. A. Almada, A. M. Tarrant, Vibrio elicits targeted transcriptional responses from copepod hosts. *FEMS Microbiol Ecol* **92**, fiw072 (2016).

34. M. Varadi *et al.*, AlphaFold Protein Structure Database in 2024: providing structure coverage for over 214 million protein sequences. *Nucleic Acids Res* **52**, D368–D375 (2024).

35. A. H. Brand, N. Perrimon, Targeted gene expression as a means of altering cell fates and generating dominant phenotypes. *Development* **118**, 401–415 (1993).

36. L. A. Perkins *et al.*, The Transgenic RNAi Project at Harvard Medical School: Resources and Validation. *Genetics* **201**, 843–852 (2015).

37. M. A. Hanson *et al.*, Synergy and remarkable specificity of antimicrobial peptides in vivo using a systematic knockout approach. *Elife* **8** (2019).

38. A. Ozturk-Colak *et al.*, FlyBase: updates to the *Drosophila* genes and genomes database. *Genetics* **227** (2024).

39. D. Hegedus, M. Erlandson, C. Gillott, U. Toprak, New insights into peritrophic matrix synthesis, architecture, and function. *Annu Rev Entomol* **54**, 285–302 (2009).

40. T. Kuraishi, O. Binggeli, O. Opota, N. Buchon, B. Lemaitre, Genetic evidence for a protective role of the peritrophic matrix against intestinal bacterial infection in *Drosophila melanogaster*. *Proc Natl Acad Sci U S A* **108**, 15966–15971 (2011).

41. B. L. Weiss, A. F. Savage, B. C. Griffith, Y. Wu, S. Aksoy, The peritrophic matrix mediates differential infection outcomes in the tsetse fly gut following challenge with commensal, pathogenic, and parasitic microbes. *J Immunol* **193**, 773–782 (2014).

42. F. Madeira *et al.*, The EMBL-EBI Job Dispatcher sequence analysis tools framework in 2024. *Nucleic Acids Res* **52**, W521–W525 (2024).

43. J. Jumper *et al.*, Highly accurate protein structure prediction with AlphaFold. *Nature* **596**, 583–589 (2021).

44. G. Wijffels *et al.*, A novel family of chitin-binding proteins from insect type 2 peritrophic matrix. cDNA sequences, chitin binding activity, and cellular localization. *J Biol Chem* **276**, 15527–15536 (2001).

45. D. Q. Hu *et al.*, The effect of group IV chitinase, HaCHT4, on the chitin content of the peritrophic matrix (PM) during larval growth and development of Helicoverpa armigera. *Pest Manag Sci* **78**, 1815–1823 (2022).

46. D. P. Leader, S. A. Krause, A. Pandit, S. A. Davies, J. A. T. Dow, FlyAtlas 2: a new version of the *Drosophila melanogaster* expression atlas with RNA-Seq, miRNA-Seq and sex-specific data. *Nucleic Acids Res* **46**, D809–D815 (2018).

47. S. Sun, Q. X. Tay, S. Kjelleberg, S. A. Rice, D. McDougald, Quorum sensing-regulated chitin metabolism provides grazing resistance to *Vibrio cholerae* biofilms. *ISME J* **9**, 1812–1820 (2015).

48. B. R. Wucher *et al.*, *Vibrio cholerae* filamentation promotes chitin surface attachment at the expense of competition in biofilms. *Proc Natl Acad Sci U S A* **116**, 14216–14221 (2019).

49. S. Nahar *et al.*, Role of Shrimp Chitin in the Ecology of Toxigenic *Vibrio cholerae* and Cholera Transmission. *Front Microbiol* **2**, 260 (2011).

50. X. Li, S. Roseman, The chitinolytic cascade in Vibrios is regulated by chitin oligosaccharides and a two-component chitin catabolic sensor/kinase. *Proc Natl Acad Sci U S A* **101**, 627–631 (2004).

51. E. Y. Markov, E. S. Kulikalova, L. Y. Urbanovich, V. S. Vishnyakov, S. V. Balakhonov, Chitin and Products of Its Hydrolysis in *Vibrio cholerae* Ecology. *Biochemistry (Mosc)* **80**, 1109–1116 (2015).

52. C. A. Klancher, S. Yamamoto, T. N. Dalia, A. B. Dalia, ChiS is a noncanonical DNA-binding hybrid sensor kinase that directly regulates the chitin utilization program in *Vibrio cholerae*. *Proc Natl Acad Sci U S A* **117**, 20180–20189 (2020).

53. S. Hang *et al.*, The acetate switch of an intestinal pathogen disrupts host insulin signaling and lipid metabolism. *Cell Host Microbe* **16**, 592–604 (2014).

54. C. P. Souza, B. C. Almeida, R. R. Colwell, I. N. Rivera, The importance of chitin in the marine environment. *Mar Biotechnol (NY)* **13**, 823–830 (2011).

55. T. J. Kirn, B. A. Jude, R. K. Taylor, A colonization factor links *Vibrio cholerae* environmental survival and human infection. *Nature* **438**, 863–866 (2005).

56. C. J. Lloyd *et al.*, A peptide-binding domain shared with an Antarctic bacterium facilitates *Vibrio cholerae* human cell binding and intestinal colonization. *Proc Natl Acad Sci U S A* **120**, e2308238120 (2023).

57. M. L. Tamplin, A. L. Gauzens, A. Huq, D. A. Sack, R. R. Colwell, Attachment of *Vibrio cholerae* serogroup O1 to zooplankton and phytoplankton of Bangladesh waters. *Appl. Environ. Microbiol.* **56**, 1977–1980 (1990).

58. B. N. Shukla, D. V. Singh, S. C. Sanyal, Attachment of non-culturable toxigenic *Vibrio cholerae* O1 and non-O1 and *Aeromonas* spp. to the aquatic arthropod *Gerris spinolae* and plants in the River Ganga, Varanasi. *FEMS Immunol. and Medical Microbiol.* **12**, 113–120 (1995).

59. T. K. Rawlings, G. M. Ruiz, R. R. Colwell, Association of *Vibrio cholerae* O1 El Tor and O139 Bengal with the Copepods Acartia tonsa and Eurytemora affinis. *Appl Environ Microbiol* **73**, 7926–7933 (2007).

60. R. S. Mueller *et al.*, *Vibrio cholerae* strains possess multiple strategies for abiotic and biotic surface colonization. *J Bacteriol* **189**, 5348–5360 (2007).

61. S. Schauer *et al.*, Dynamics of *Vibrio cholerae* abundance in Austrian saline lakes, assessed with quantitative solid-phase cytometry. *Environ Microbiol* **17**, 4366–4378 (2015).

62. J. W. Turner, L. Malayil, D. Guadagnoli, D. Cole, E. K. Lipp, Detection of Vibrio parahaemolyticus, Vibrio vulnificus and *Vibrio cholerae* with respect to seasonal fluctuations in temperature and plankton abundance. *Environ Microbiol* **16**, 1019–1028 (2014).

63. Y. G. Wang, L. C. Tseng, M. Lin, J. S. Hwang, Vertical and geographic distribution of copepod communities at late summer in the Amerasian Basin, Arctic Ocean. *PLoS One* **14**, e0219319 (2019).

64. M. Gluchowska *et al.*, Variations in the structural and functional diversity of zooplankton over vertical and horizontal environmental gradients en route to the Arctic Ocean through the Fram Strait. *PLoS One* **12**, e0171715 (2017).

65. Z. Zhang *et al.*, Spatio-Temporal Variations of Zooplankton and Correlations with Environmental Parameters around Tiaowei Island, Fujian, China. *Int J Environ Res Public Health* **19** (2022).

66. V. Venkataramana, L. Gawade, M. D. Bharathi, V. Sarma, Role of salinity on zooplankton assemblages in the tropical Indian estuaries during post monsoon. *Mar Pollut Bull* **190**, 114816 (2023).

67. G. Boldrocchi, Y. Moussa Omar, D. Rowat, R. Bettinetti, First results on zooplankton community composition and contamination by some persistent organic pollutants in the Gulf of Tadjoura (Djibouti). *Sci Total Environ* **627**, 812–821 (2018).

68. P. Mrak, U. Bogataj, J. Strus, N. Znidarsic, Cuticle morphogenesis in crustacean embryonic and postembryonic stages. *Arthropod Struct Dev* **46**, 77–95 (2017).

69. M. R. Sochard, D. F. Wilson, B. Austin, R. R. Colwell, Bacteria associated with the surface and gut of marine copepods. *Appl Environ Microbiol* **37**, 750–759 (1979).

70. B. Moussian, The apical plasma membrane of chitin-synthesizing epithelia. *Insect Sci* **20**, 139–146 (2013).

71. C. Rose *et al.*, An investigation into the protein composition of the teneral Glossina morsitans morsitans peritrophic matrix. *PLoS Negl Trop Dis* **8**, e2691 (2014).

72. C. A. Klancher *et al.*, The ChiS-Family DNA-Binding Domain Contains a Cryptic Helix-Turn-Helix Variant. *mBio* **12** (2021).

73. E. Wong *et al.*, The *Vibrio cholerae* colonization factor GbpA possesses a modular structure that governs binding to different host surfaces. *PLoS Pathog* **8**, e1002373 (2012).

74. J. S. Loose, Z. Forsberg, M. W. Fraaije, V. G. Eijsink, G. Vaaje-Kolstad, A rapid quantitative activity assay shows that the *Vibrio cholerae* colonization factor GbpA is an active lytic polysaccharide monooxygenase. *FEBS Lett* **588**, 3435–3440 (2014).

75. K. A. Syed *et al.*, The *Vibrio cholerae* flagellar regulatory hierarchy controls expression of virulence factors. *J Bacteriol* **191**, 6555–6570 (2009).

76. W. Song, J. A. Veenstra, N. Perrimon, Control of Lipid Metabolism by Tachykinin in *Drosophila*. *Cell Rep* **30**, 2461 (2020).

77. A. J. Haugo, P. I. Watnick, *Vibrio cholerae* CytR is a repressor of biofilm development. *Mol Microbiol* **45**, 471–483 (2002).

78. A. Dobin *et al.*, STAR: ultrafast universal RNA-seq aligner. *Bioinformatics* **29**, 15–21 (2013).

79. R. Patro, G. Duggal, M. I. Love, R. A. Irizarry, C. Kingsford, Salmon provides fast and bias-aware quantification of transcript expression. *Nat Methods* **14**, 417–419 (2017).

80. M. I. Love, W. Huber, S. Anders, Moderated estimation of fold change and dispersion for RNA-seq data with DESeq2. *Genome Biol* **15**, 550 (2014).

81. M. Cornwell *et al.*, VIPER: Visualization Pipeline for RNA-seq, a Snakemake workflow for efficient and complete RNA-seq analysis. *BMC Bioinformatics* **19**, 135 (2018).

**Acknowledgements**

This work was supported by NIH R01AI158247 and NIH R01AI162701 to P.I.W. and NIH F31DK130254 to D. B. Anti-TK antibodies were generously provided by Jan Veenstra and AMP-deficient flies and the corresponding parental strain were generously provided by Bruno Lemaitre. The TK-Gal4 and NP1-Gal4 (Myo1A-Gal4) driver flies were kind gifts from Norbert Perrimon. Stocks obtained from the Bloomington *Drosophila* Stock Center (NIH P40OD018537) were used in this study. Microscopy images were acquired at the Microscopy Resources on the North Quad (MicRoN) core at Harvard Medical School. We thank Paola Montero Lopis and Praju Vikas Anekal at the MicRoN core for providing expertise with image acquisition and quantification.

**Author contributions statement.** D.B. and P.I.W. conceived the project. D.B., T.F.P. and P.I.W. designed the experiments. D.B. and T.F.P. contributed equally. D.B., T.F.P., L.F. and S. H. performed the experiments and acquired the data. D.B. T.F.P., L.F and P.I.W. analyzed the data and interpreted the results. T.F.P., D. B. and P.I.W. revised the work. D. B, T. F. P., and P.I.W. wrote the manuscript with input from all authors. P.I.W. supervised the project and acquired funding. All authors reviewed and approved the final manuscript.

**Competing interests statement.** The authors declare no competing interests.

**Figure Legends:**

**Figure 1: Knockdown of IMD and Tk signaling in enteroendocrine cells decreases *V. cholerae* colonization of the arthropod intestine, while knockdown in enterocytes increases colonization.** (A) Schematic of the different regions of the *Drosophila* intestine including the foregut (FG), midgut (MG), hindgut (HG), and rectum (R). The midgut is comprised of the anterior midgut (AMG), the middle midgut (MMG), and the posterior midgut (PMG). Green boxes indicate the regions of the AMG and PMG where lipid content is assessed. Created in BioRender. Watnick, P. (2026) https://BioRender.com/ g94m850. (B) IMD pathway activation signals and signaling in Tk-expressing enteroendocrine cells of the AMG. Created in BioRender. Watnick, P. (2026) https://BioRender.com/t24m790. Quantification of *V. cholerae* intestinal colonization of (C) enterocyte driver (NP1>) (n = 18) and NP1>*Rel*$^{RNAi}$ (NP1>*Rel*$^{RNAi}$) flies (n = 20) (p-value = 0.002), (D) Tk+ enteroendocrine cell driver (Tk>) and Tk>*Tk*$^{RNAi}$ flies, (n = 8, each) (E) NP1> and NP1>*TkR99D*$^{RNAi}$ flies (p-value = 0.0137), (F) NP1> and NP1>*Rel*$^{RNAi}$ flies (n=8, each) (p-value < 0.0001), and (G) parental *w*$^{1118}$ (CTL) and flies with 10 AMPs deleted (ΔAMP) (n = 8, each) (p-value = 0.002). Flies were fed *V. cholerae* for 48 hours, and non-adherent bacteria were then washed out by feeding on PBS for 24 hours. A two-tailed student's t test was applied to log-transformed data to calculate significance. **** p<0.0001, *** p<0.001, ** p<0.01, * p<0.05. Source data are provided as a source data file.

**Figure 2: RNA-seq comparing transcription in the intestines of Tk> and Tk>*Tk*$^{RNAi}$ flies reveals differential regulation of genes involved in the innate immune response, lipid catabolism, and chitin binding.** (A) RNA-seq was performed on the intestines of Tk> and Tk>*Tk*$^{RNAi}$ flies using biological triplicates. Volcano plot showing

the $log_2$fold-change (FC) and the p-value adjusted for multiple comparisons (padj) for gene expression in Tk>*Tk*$^{RNAi}$/Tk> conditions. The vertical dotted lines indicate a 2-fold change. Colored points meet the threshold ≥ 2-fold change and padj < 0.05. Significantly regulated genes involved in innate immunity are shown in dark green (including *Defensin* or *Def*), those involved in lipid catabolism are shown in brown (including *Lip3* and *CG17192*), and those involved in chitin binding are shown in purple. Peri-15A and B are shown in bright green. (B) qRT-PCR quantification of the indicated genes in the intestines of Tk> and Tk>*Tk*$^{RNAi}$ flies. These genes were also significantly differentially regulated in the RNA-seq experiment. The mean of biological triplicates is shown. Error bars indicate the standard deviation. A two-tailed Welch's t test was used to evaluate significance. (p-value = 0.0275) (C) Fluorescence images showing DAPI and BODIPY (Lipid) staining in the anterior midgut (AMG) and posterior midgut (PMG) of the indicated fly genotypes. Scale bars, 50 μM. (D) Quantification of total fluorescence in the AMG and PMG of the indicated flies incubated with BODIPY. Six intestines were evaluated. The mean is shown. A two-tailed students' t-test was used to evaluate significance. **** p<0.0001, * p<0.05, ns not significant. Source data are provided as a source data file.

**Figure 3: Homologs peritrophin-15a and -15b are most highly expressed in enteroendocrine cells of the *Drosophila* midgut and regulated by the enteroendocrine IMD pathway and Tk.** (A) Alignment of the amino acid sequences of Peritrophin-15a (Peri-15a) and Peritrophin-15b (Peri-15b) using Clustal Omega. The sequences are 45% identical and 58% similar. (B) Alpha fold generated structures of Peri-15a and Peri-15b. The N-terminal helices representing approximately residues 1-22 are predicted signal peptides, while residues 31-92 in Peri-15a and 38-89 in Peri-15b

are predicted type 2 chitin binding domains. (C) Expression of the three midgut peritrophins, Peritrophin A, 15a, and 15b in the 5 regions of the midgut (R1-R5) and midgut cell types including stem cells (ISC), enteroblasts (EB), enterocytes (EC), enteroendocrine cells (EEC) and ventral muscle (VM). Data is from the flygutseq database (from http://flygutseq.buchonlab.com). (D and E) qRT-PCR analysis of intestinal expression of Peri-15a in the the indicated flies. The mean of biological triplicates is shown. Error bars represent the standard deviation. A two-tailed student's t test was used to assess statistical significance. (D p-value = 0.0368, E p-value = 0.0004) *** p<0.001, * p<0.05. Source data are provided as a source data file.

**Figure 4: Peri-15a promotes *V. cholerae* colonization of the arthropod intestine without impacting expression of Tk or AMPs.** qRT-PCR analysis of (A)*Tk* and (B) *Peri-15a* transcription in the intestines of *yw* flies fed either LB alone (CTL) or inoculated with *V. cholerae strain* C6706str2 (*Vc*). No washout was performed. The mean of biological triplicates is shown. Error bars represent the standard deviation. Significance was calculated using a two-tailed student's t test. (A p-value = 0.0172, B p-value = 0.0453). (C) *V. cholerae* colonization of the intestines of flies with the indicated genotypes. Data were log-transformed. The mean of eight intestines is shown. Significance was calculated using a two-tailed Welch's t test (p-value = 0.0004). (D) qRT-PCR analysis of transcription of *Peri-15, Tk,* or *Def* in the intestines of pros> or pros>*Peri-15a*$^{RNAi}$ flies. The mean of biological triplicates is shown. Error bars represent the standard deviation. Significance was calculated using a two-tailed student's t test (Peri-15a p-value = 0.0451; Tk p- value = 0.7681, Def p-value = 0.5943). (E) Quantitation of BODIPY (Lipid) staining and Tk immunofluorescence in the anterior midgut (AMG) (Tk+ p-value = 0.0106, fluorescence p-value = 0.7542) and posterior

midgut (PMG) (Tk+ p-value = 0.1204, fluorescence p-value = 0.9139) of the indicated fly genotypes (pros> control n = 10, pros>*Peri-15a*$^{RNAi}$ n = 9). The mean of sampled intestines is shown. Significance was calculated using a two-tailed student's t test. ***p < 0.001, * p < 0.05, ns not significant. Source data are provided as a source data file.

**Figure 5: Transcriptional activation of Peritrophin-15a by 20-hydroxyecdysone increases *V. cholerae* colonization of the arthropod intestine.** (A) qRT-PCR analysis of transcription of the genes tachykinin (*Tk*) and Peritrophin-15a (*Peri-15a*) in *yw* flies fed LB broth (CTL) or LB broth supplemented with 20-hydroxyecdysone (20E). The mean of biological triplicates is shown. Error bars represent the standard deviation. For *Tk*, a two-tailed student's t-test was used to assess significance (p-value 0.0065). For *Peri-15a*, a lognormal student's t test was used to assess significance (p-value = 0.0453). *V. cholerae* colonization of the intestines of (B) *yw* or (C) pros> and pros>*Peri-15a*$^{RNAi}$ flies fed LB alone or supplemented with 20-hydroxyecdysone (20E). The mean of three biological is shown. In (B) 16 flies were used per condition, and a two-tailed student's t test was used to assess significance (p-value = 0.0067). In (C) at least 8 flies per genotype were used and a Welch's ANOVA with Dunnett's T3 multiple comparisons test was applied to assess significance (in order: p-value = 0.0111, p-value = 0.0011, p-value = 0.0075, p-value = 0.4391). **** p<0.0001, *** p<0.001, * p<0.05, ns not significant. Source data are provided as a source data file.

**Figure 6: Peritrophic matrix continuity is not correlated with *V. cholerae* adhesion.** (A) Expression of Chitinase 4 (Cht4) and Chitinase 9 (Cht9) in different intestinal cell types (ISC intestinal stem cells, EB enteroblasts, EC enterocytes, EEC enteroendocrine cells). database (from http://flygutseq.buchonlab.com/). (B) *V. cholerae* colonization of an enterocyte driver-only fly (NP1>) and a fly with knockdown of the indicated chitinases

in enterocytes. Bars represent the mean of eight biological replicates per genotype. An ordinary ANOVA with a Dunnett's multiple comparisons test was performed on $\log_{10}$ transformed data to assess significance (in order: p-value = 0.0350, p-value = 0.9830). (C) qRT-PCR measurements of *Cht4*, *Tk, Def*, and *Peri-15a* transcription in the intestines of flies of the indicated genotypes. The mean of three biological replicates is shown. Error bars represent the standard deviation. Significance was assessed using a Welch's t test for *Cht4* and a two-tailed student's t test for all others (Ch4 p-value = 0.0047, Tk p-value = 0.0118, Def p-value = 0.0032, Peri-15a p-value = 0.0042). Source data are provided as a source data file.

**Figure 7: Peri-15a knockdown does not impact PM permeability.** Imaging of the PMG of flies of the indicated fly genotypes fed either 40 kDa or 500 kDa FITC-labelled dextran. A representative micrograph of 6 replicates each is shown for $w^{1118}$ flies fed 40kDa dextran and $w^{1118}$ flies fed 500kDa. For $Crys^{MB08319}$ fed 40kDa dextran and $Crys^{MB08319}$ fed 500kDa dextran, micrographs of a gut with leakage are shown. Leakage was observed for 6/7 $Crys^{MB08319}$ flies fed 40kDa dextran and 4/5 flies fed 500kDa dextran. Below representative micrographs are shown for Np1> (n=5 and n=5) and Np1>$Cht4^{RNAi}$ (n=3 and n=3) flies fed 40kDa or 500 kDa dextran and pros> (n=4 and n=5) and pros>Peri-$15a^{RNAi}$ (n=8 and n=6) flies fed 40kDa or 500 kDa dextran. Additional pros> and pros>Peri-$15a^{RNAi}$ micrographs are shown in Fig S2. Measure bars 50 µm. Source data are provided as a source data file.

**Figure 8: The *V. cholerae* master regulator of chitin metabolism, ChiS, decreases *V. cholerae* colonization of the arthropod intestine in a Peritrophin-15a-dependent fashion.** (A) qRT-PCR analysis of transcript abundance of the *V. cholerae* genes *chiA1* and *chiA2* in the intestines of $y^1w^1$ control flies. The mean of tested biological replicates

is shown. Error bars represent the standard deviation. Significance was calculated using a two-tailed Mann-Whitney test (chiA1 p-value = 0.0293, chiA2 p-value = 0.0027). Colonization of (B) $w^{1118}$ parental flies (CTL) and flies with deletion of 10 genes encoding antimicrobial peptides (ΔAMP) with either wild-type *V. cholerae* (WT) (n = 24, n = 23) or a Δ*chiS* mutant (n = 24, n = 24). The mean of $\log_{10}$ transformed data is shown. A two-tailed t test (in order: p-value = 0.0223, p-value = 0.0195). Colonization of (C) Tk> driver only and Tk>$Tk^{RNAi}$ flies or (D) pros> driver-only and pros>$Peri15a^{RNAi}$ flies with the indicated *V. cholerae* strains. Eight flies were quantified for each condition. The mean of $\log_{10}$ transformed data is shown. An ordinary one-way ANOVA with Dunnett's multiple comparisons test was used to assess significance (in order: (C) p-value = 0.0017, p-value = 0.0399, p-value = 0.0008; (D) p-value < 0.0001, p-value = 0.0145, p-value < 0.0001). **** p,0.0001, ** p<0.01, * p<0.05, ns not significant. Source data are provided as a source data file.

**Figure 9: Structural homologs of Peri-15a are found in cyanobacteria, fungi, rotifers, copepods and marine insects**. Alpha fold AFDB50, AFDB Fold, and AFDB50MMseq2 were used to find structural homologs of *Drosophila* Peri-15a. The structures of homologs found in insect vectors, copepods, a rotifer, and a cyanobacterium are shown.



*Vibrio cholerae* can be found in the marine environment in close association with marine arthropods. Using Drosophila melanogaster as a model arthropod, authors report that the host chitin-binding protein Peritrophin-15a increases *V. cholerae* colonization of the arthropod gut.

**Peer review information**: *Nature Communications* thanks the anonymous reviewers for their contribution to the peer review of this work. A peer review file is available.

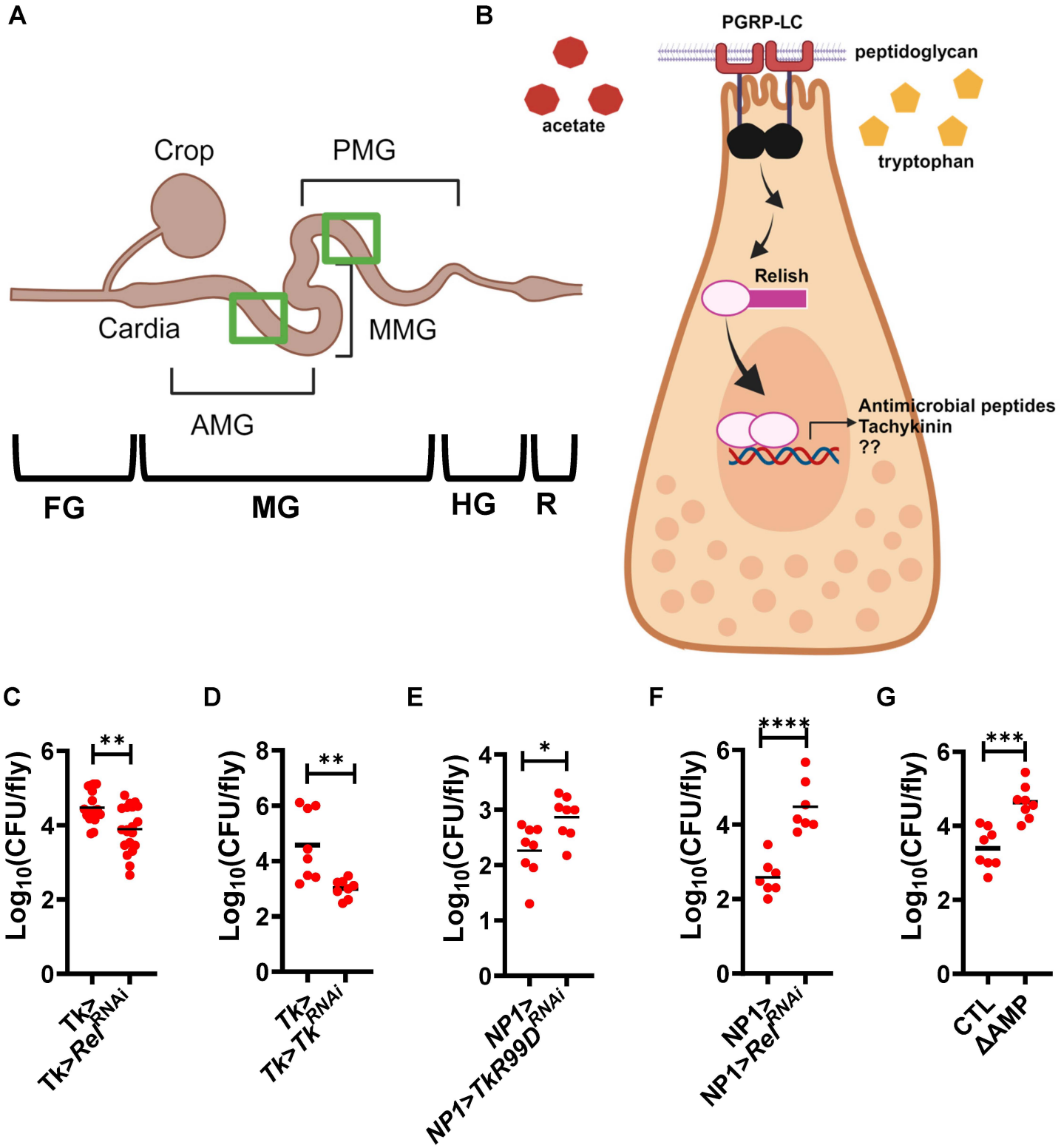
A
Crop
PMG
Cardia
MMG
AMG
FG
MG
HG
R
B
acetate
PGRP-LC
peptidoglycan
tryptophan
Relish
Antimicrobial peptides
Tachykinin
??
C
D
E
F
G
Log10(CFU/fly)
Tk>
Tk>Rel^RNAi
Tk>Tk^RNAi
NP1>
NP1>TkR99D^RNAi
NP1>Rel^RNAi
CTL
ΔAMP

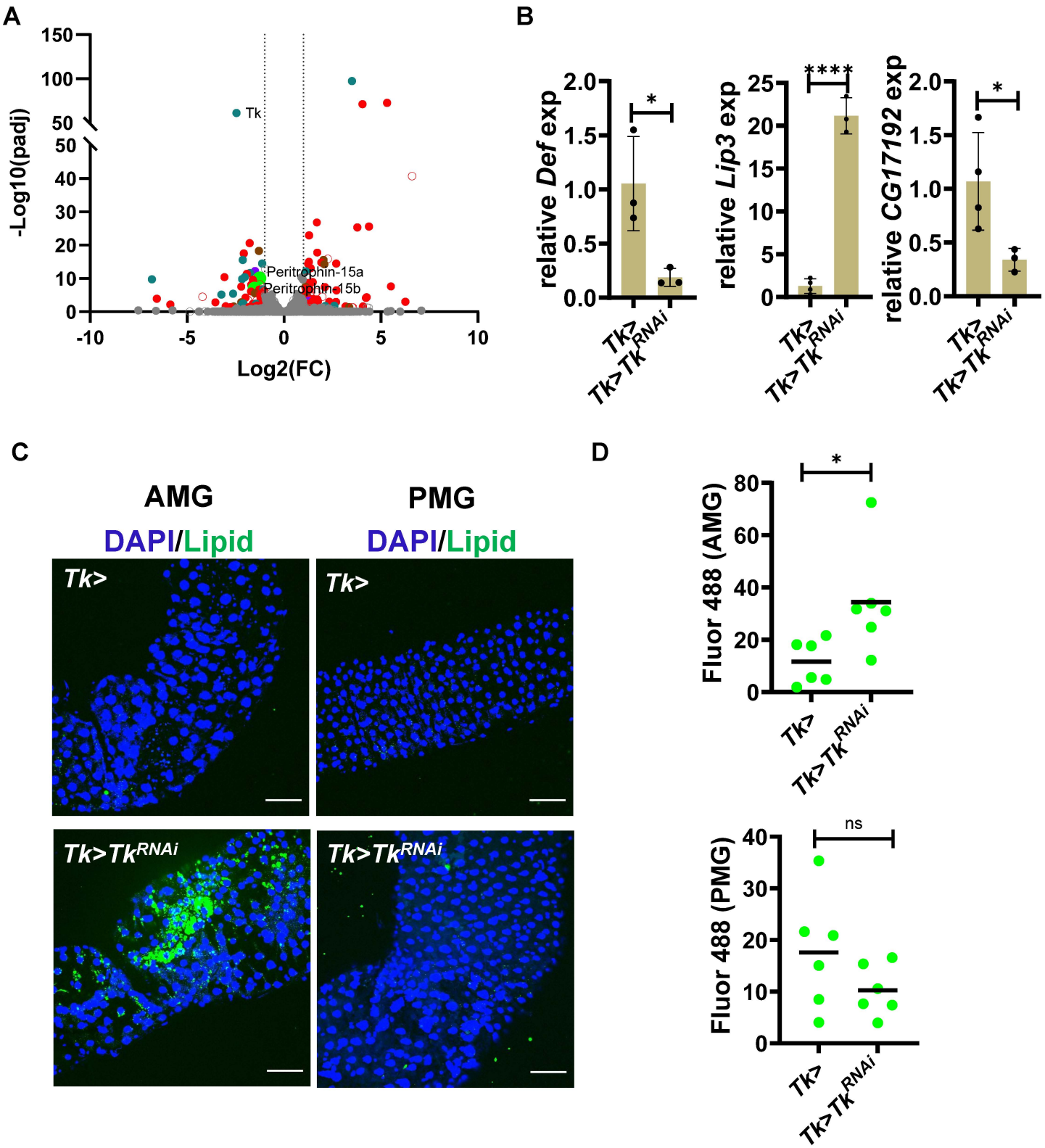
A
-Log10(padj)
Log2(FC)
Tk
Peritrophin-15a
Peritrophin-15b
B
relative Def exp
relative Lip3 exp
relative CG17192 exp
Tk>
Tk>Tk^RNAi
C
AMG
PMG
DAPI/Lipid
Tk>
Tk>Tk^RNAi
D
Fluor 488 (AMG)
Fluor 488 (PMG)
ns

A

```
Peri-15a    MKSALLLICLAFFVALLSTGNACDPNSDNQPDCSDASNVQTNIRNFWDPTRYWWCESSTS
Peri-15b    MKAALVLLFLTLCVAIYADLD-CNPDGNGEPDCVGRSGEIS--RDFWDPTHYWQC-SSTG
            **:**:*: *:: **: :  : *:*:.:.:*** . *.  :  *:*****.**.* ***.

Peri-15a    TATAVLCPLSTGFDPTKKECVSWSEWSWTAYC-----
Peri-15b    QAELVACEQNTGFDPKTGSCVDWSVWQWYPPCSEAST
             *  * *  .******.. .**.** *.* . *
```

B

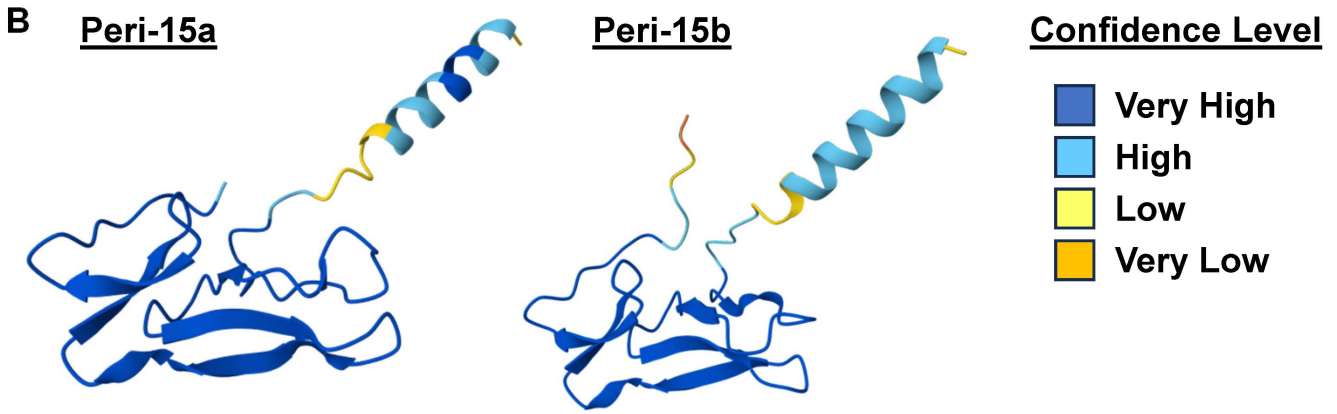


C

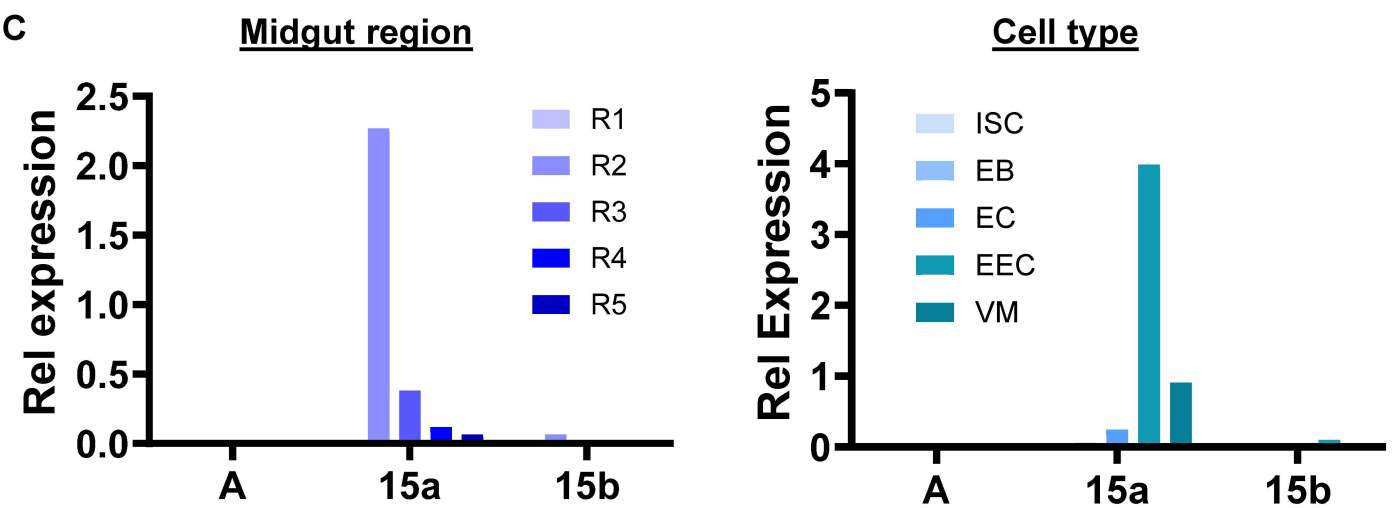


D

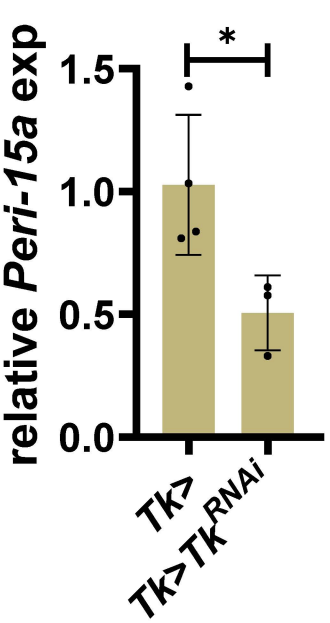


E

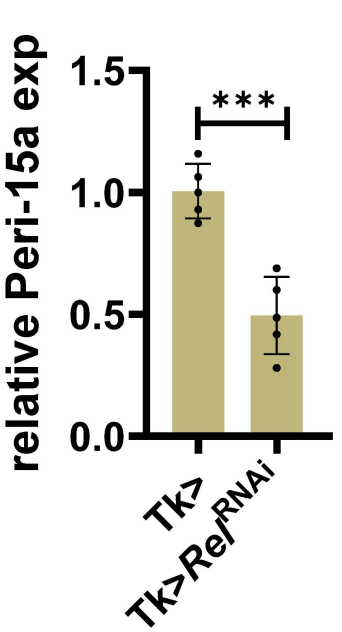

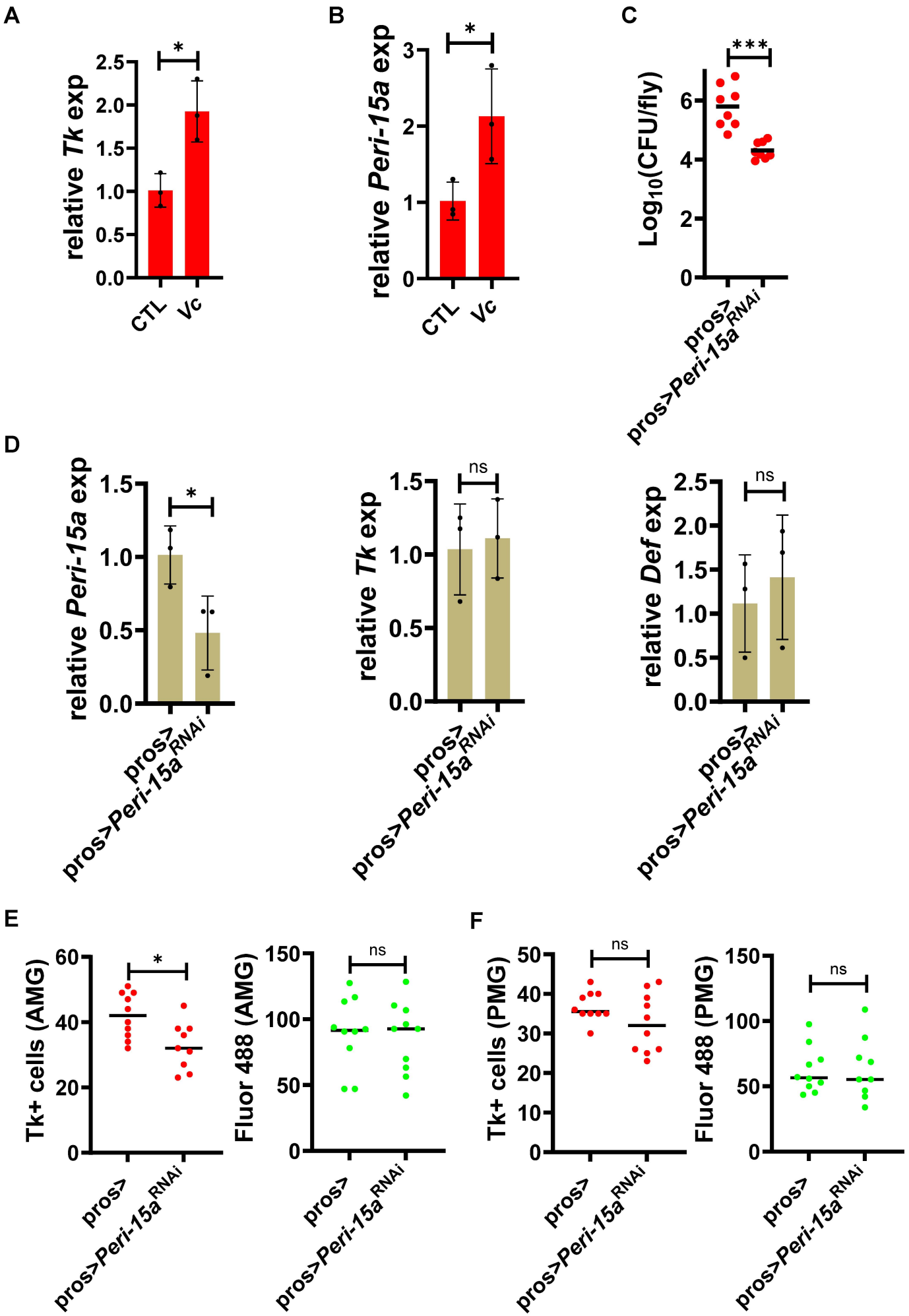
A
relative Tk exp
2.5
2.0
1.5
1.0
0.5
0.0
*
CTL
Vc
B
relative Peri-15a exp
3
2
1
0
*
CTL
Vc
C
Log10(CFU/fly)
6
4
2
0
***
pros>
pros>Peri-15a RNAi
D
relative Peri-15a exp
1.5
1.0
0.5
0.0
*
pros>
pros>Peri-15a RNAi
relative Tk exp
1.5
1.0
0.5
0.0
ns
pros>
pros>Peri-15a RNAi
relative Def exp
2.5
2.0
1.5
1.0
0.5
0.0
ns
pros>
pros>Peri-15a RNAi
E
Tk+ cells (AMG)
60
40
20
0
*
pros>
pros>Peri-15a RNAi
Fluor 488 (AMG)
150
100
50
0
ns
pros>
pros>Peri-15a RNAi
F
Tk+ cells (PMG)
50
40
30
20
10
0
ns
pros>
pros>Peri-15a RNAi
Fluor 488 (PMG)
150
100
50
0
ns
pros>
pros>Peri-15a RNAi

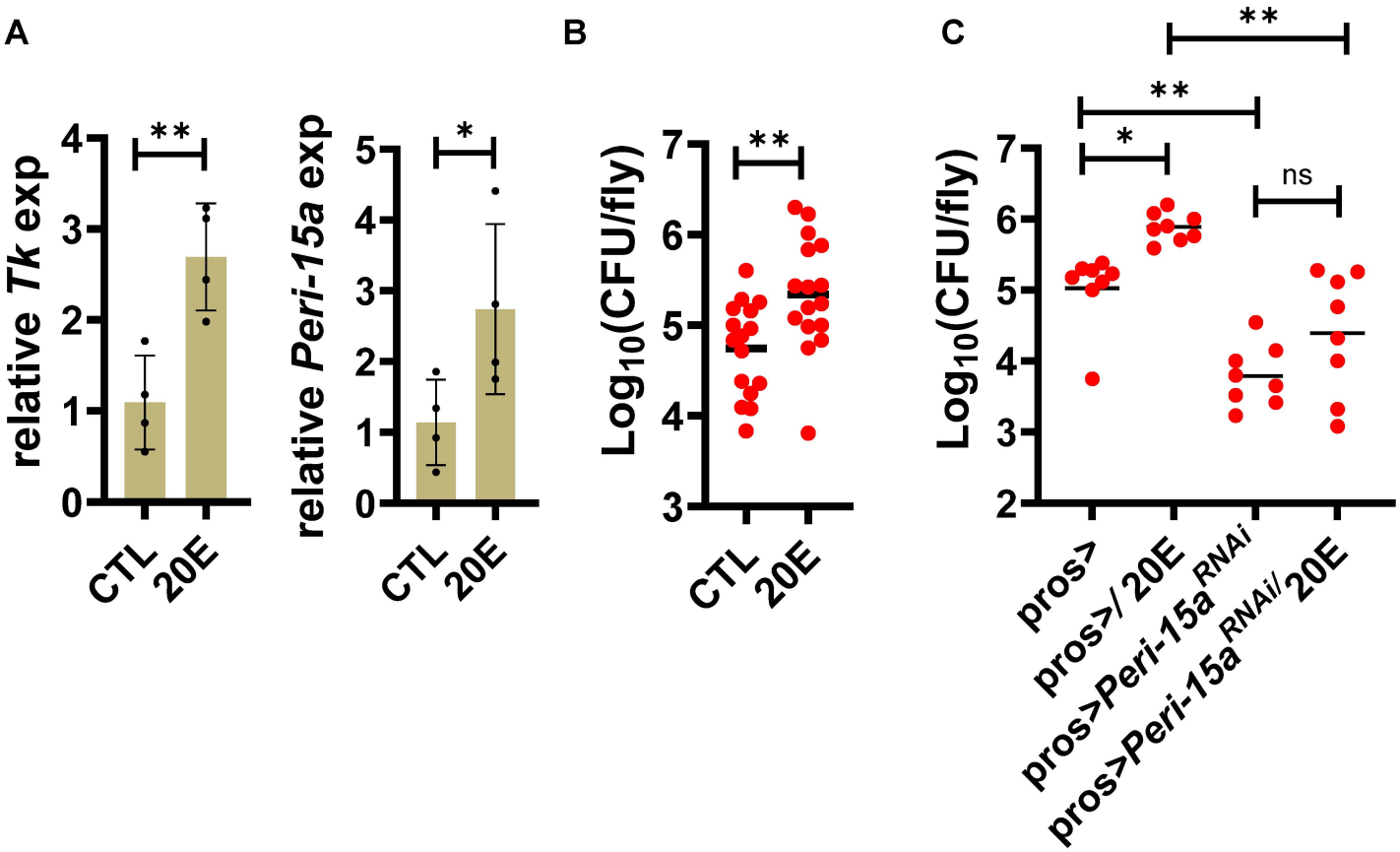
A
relative Tk exp
**
CTL
20E
relative Peri-15a exp
*
CTL
20E
B
Log10(CFU/fly)
**
CTL
20E
C
Log10(CFU/fly)
**
*
**
ns
pros>
pros>/ 20E
pros>Peri-15a RNAi
pros>Peri-15a RNAi/ 20E

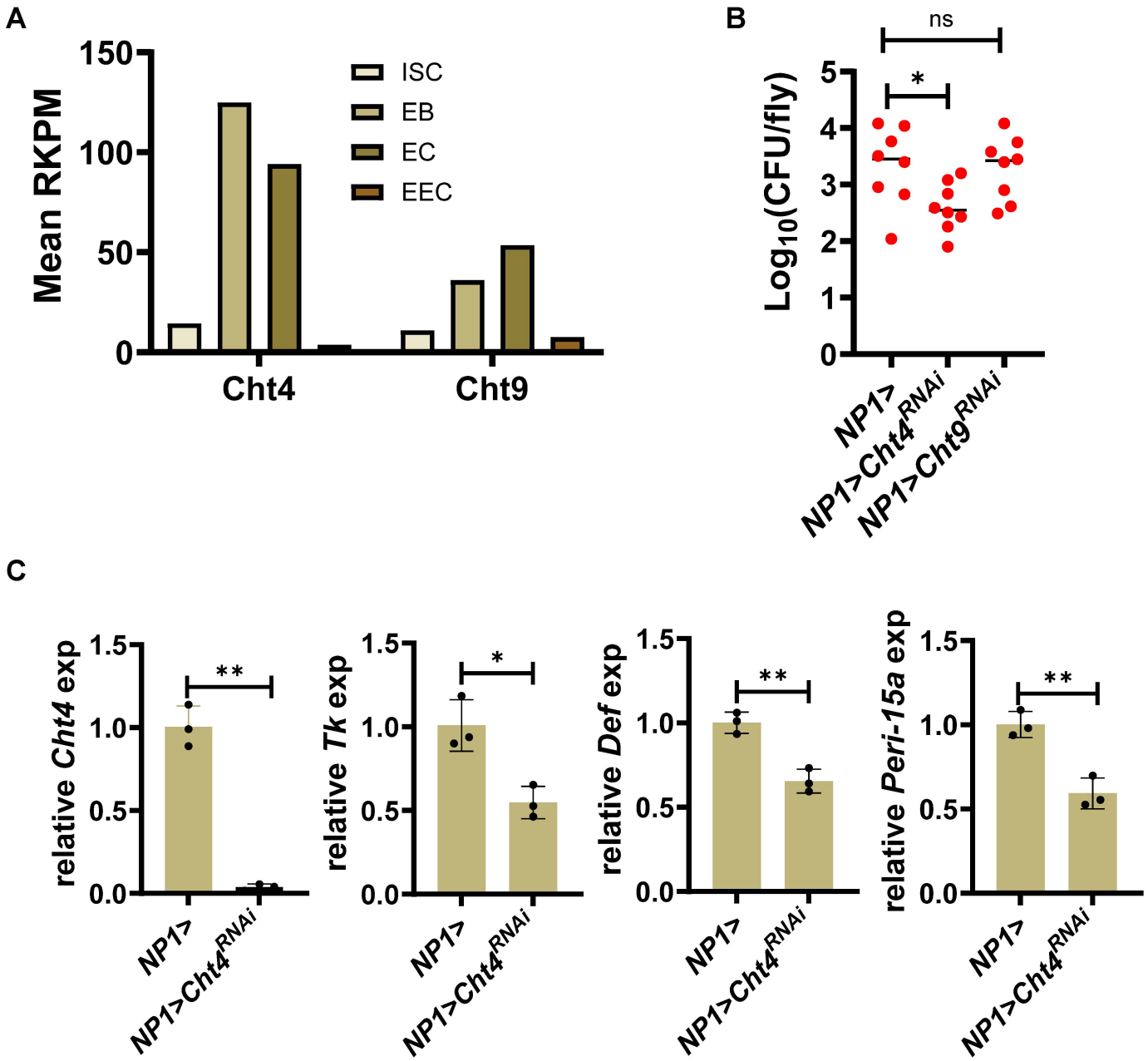
A
Mean RKPM
150
100
50
0
ISC
EB
EC
EEC
Cht4
Cht9
B
ns
*
Log10(CFU/fly)
5
4
3
2
1
0
NP1>
NP1>Cht4RNAi
NP1>Cht9RNAi
C
relative Cht4 exp
relative Tk exp
relative Def exp
relative Peri-15a exp
1.5
1.0
0.5
0.0
**
*
NP1>
NP1>Cht4RNAi

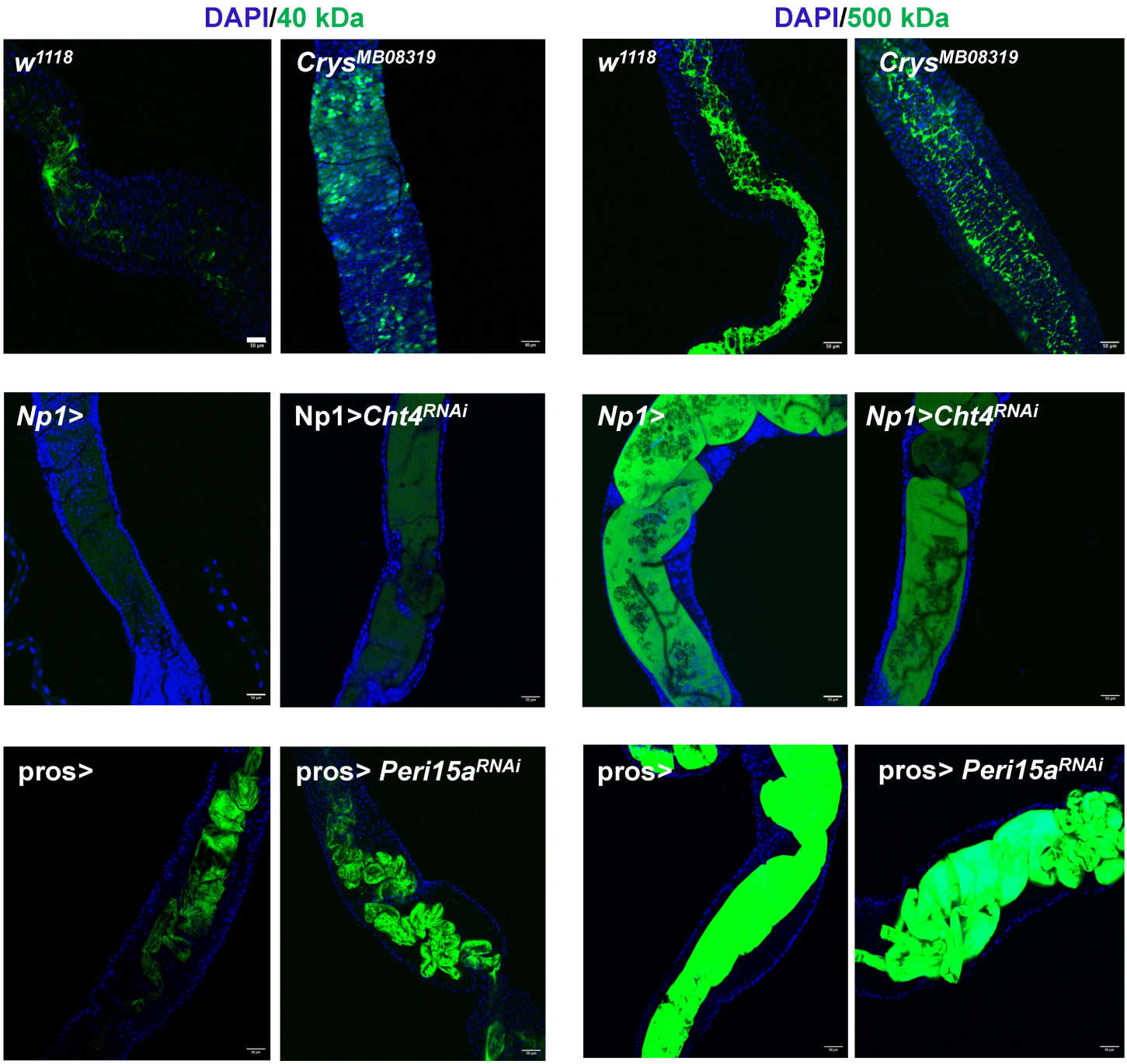
DAPI/40 kDa
DAPI/500 kDa
w1118
CrysMB08319
w1118
CrysMB08319
Np1>
Np1>Cht4RNAi
Np1>
Np1>Cht4RNAi
pros>
pros> Peri15aRNAi
pros>
pros> Peri15aRNAi

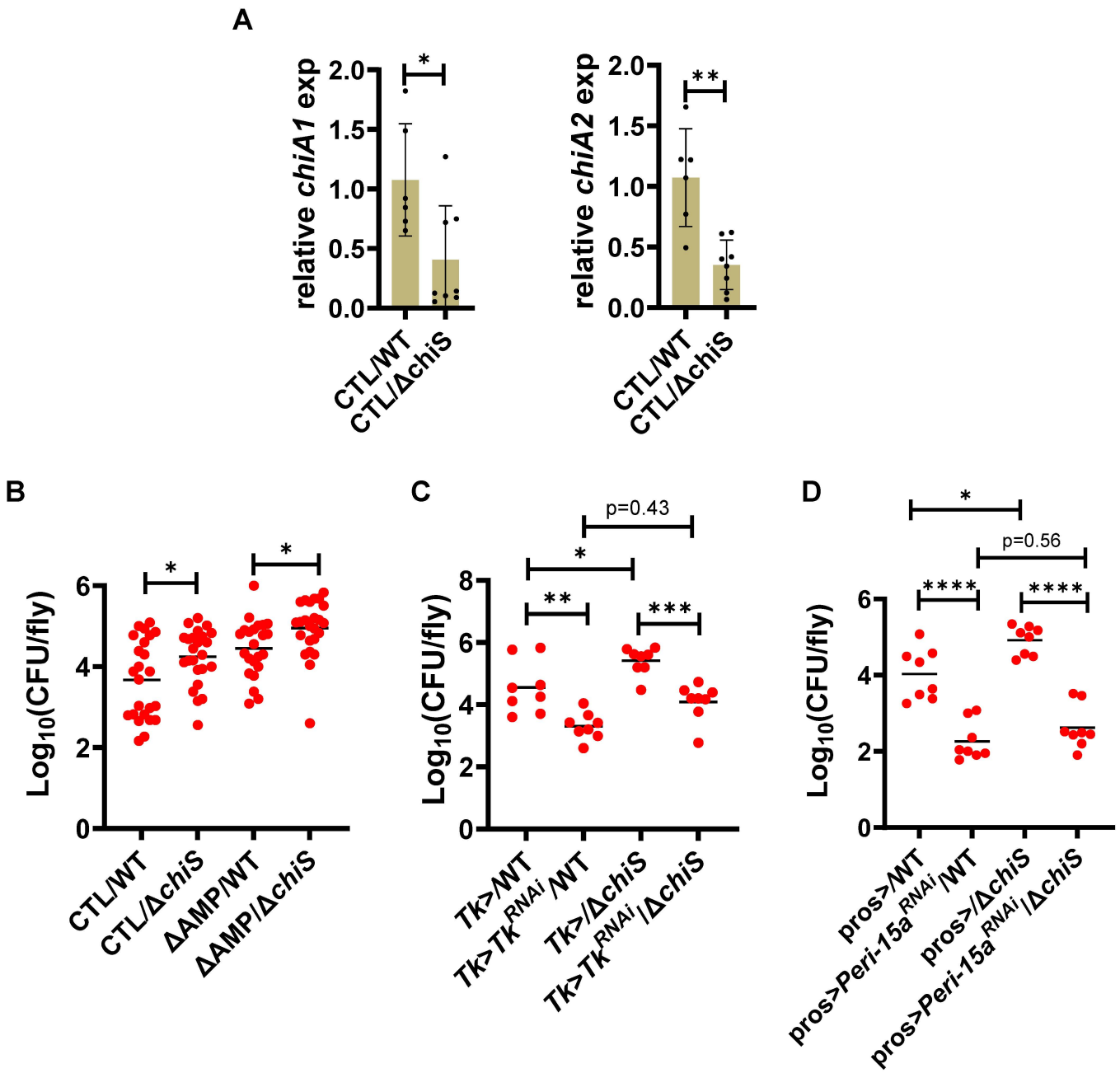
A
relative chiA1 exp
2.0
1.5
1.0
0.5
0.0
*
CTL/WT
CTL/ΔchiS
relative chiA2 exp
2.0
1.5
1.0
0.5
0.0
**
CTL/WT
CTL/ΔchiS
B
Log10(CFU/fly)
6
4
2
0
*
*
CTL/WT
CTL/ΔchiS
ΔAMP/WT
ΔAMP/ΔchiS
C
Log10(CFU/fly)
8
6
4
2
0
p=0.43
*
**
***
Tk>/WT
Tk>Tk^RNAi/WT
Tk>/ΔchiS
Tk>Tk^RNAi/ΔchiS
D
Log10(CFU/fly)
6
4
2
0
*
p=0.56
****
****
pros>/WT
pros>Peri-15a^RNAi/WT
pros>/ΔchiS
pros>Peri-15a^RNAi/ΔchiS

***Drosophila melanogaster***
**Peri-15a**

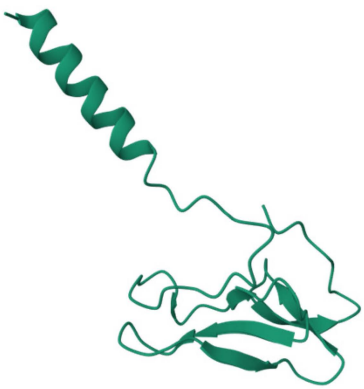

***Musca domestica***
**House fly**

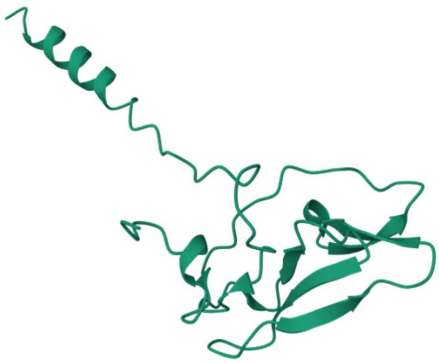

***Glossinia fuscipes***
**Tse tse fly**

***Aedes albopictus***
**mosquito**

***Clunio marius***
**Marine non-biting midge**

***Lepeophtheirus salmonis***
**Salmon louse, marine copepod**

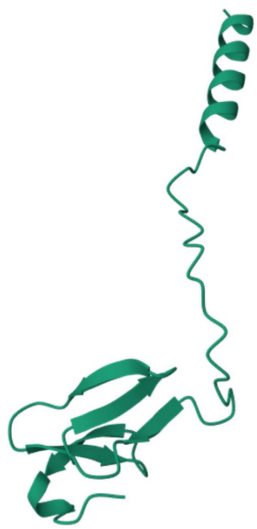

***Tigriopus californicus***
**Marine copepod**

***Didymodactylos carnosus***
**rotifer**

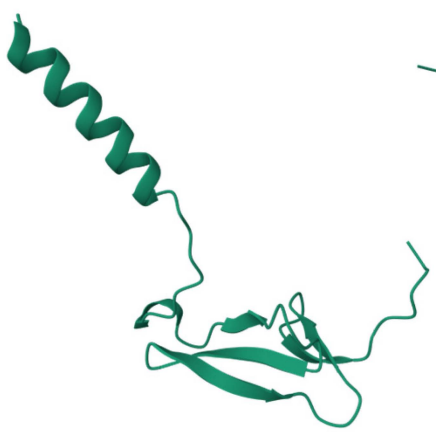

***Nostoc sp peltigera membranacea***
**Cyanobacterium**